

# Trigonal-prismatic and Octahedral Hexaruthenium Boride Clusters: Molecular Structures of $[N(PPh_3)_2][Ru_6H_2(CO)_{18}B]$ , $[Ru_6(CO)_{17}B\{AuP(C_6H_4Me-2)_3\}]$ , $[Ru_6H(CO)_{16}B\{Au(PPh_3)\}_2]$ and $[Ru_6(CO)_{16}B\{Au(PPh_3)\}_3]$

Catherine E. Housecroft,\*<sup>a</sup> Dorn M. Matthews,<sup>a</sup> Anne Waller,<sup>a</sup> Andrew J. Edwards<sup>b</sup> and Arnold L. Rheingold \*<sup>b</sup>

<sup>a</sup> University Chemical Laboratory, Lensfield Road, Cambridge CB2 1EW, UK

<sup>b</sup> Department of Chemistry, University of Delaware, Newark DE 19716, USA

The reaction of the  $[N(PPh_3)_2]^+$  salt of  $[Ru_3(CO)_9(B_2H_5)]^-$  with  $[Ru_3(CO)_{10}(NCMe)_2]$  yielded both the octahedral  $[Ru_6(CO)_{17}B]^-$  **1** and trigonal-prismatic  $[Ru_6H_2(CO)_{18}B]^-$  **2** boride cluster anions. This result indicates that the choice of the trigonal-prismatic *versus* octahedral cage is not determined by the size of the interstitial atom. The salt  $[N(PPh_3)_2][Ru_6H_2(CO)_{18}B]$  has been structurally characterised. The reactions of anions **1** and **2** with  $[AuCl(PPh_3)]$ ,  $[AuCl\{P(C_6H_4Me-2)_3\}]$ ,  $\{[(Ph_3P)Au]_3O\}[BF_4]$  and  $\{[(2-MeC_6H_4)_3PAu]_3O\}[BF_4]$  have been studied and the distribution of the products  $[Ru_6(CO)_{16}B\{Au(PR_3)\}]$ ,  $[Ru_6H(CO)_{16}B\{Au(PR_3)\}_2]$  and  $[Ru_6(CO)_{16}B\{Au(PR_3)\}_3]$  as a function of R (Ph or 2-MeC<sub>6</sub>H<sub>4</sub>) and of the starting cluster has been examined. The trigold derivatives are best prepared by treating the octahedral anion **1** with  $\{[(Ph_3P)Au]_3O\}^+$ . Single-crystal X-ray crystallography has confirmed that each of the gold(I) phosphine derivatives has an octahedral Ru<sub>6</sub>B core.

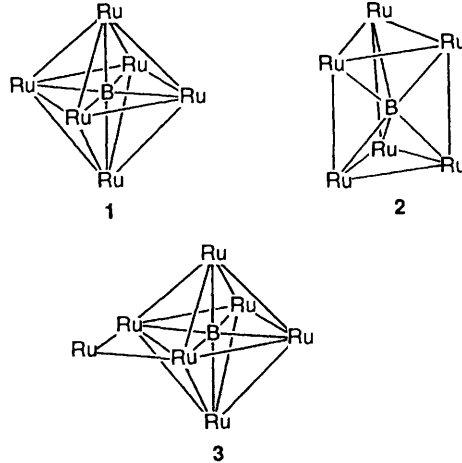
Transition-metal clusters which encapsulate p-block atoms<sup>1–5</sup> are well documented but carbide clusters predominate.<sup>1–3</sup> In terms of regular, closed polyhedra, a hexametallic framework is typically either an octahedron (86 valence electrons) or, less often, a trigonal prism (90 valence electrons). In cobalt and rhodium chemistry the trigonal-prismatic cluster carbide is represented.<sup>3,6–11</sup> However, within the Group 8 triad, the trend observed for hexametallic clusters incorporating p-block elements has tended to suggest that a first-row atom (B,<sup>4,12–15</sup> C,<sup>1–3</sup> N<sup>4,5</sup>) prefers to reside within an octahedral M<sub>6</sub> cage, while the trigonal-prismatic cage is observed when the interstitial atom is a larger p-block atom, e.g. phosphorus.<sup>4,16,17</sup> Recently,<sup>18</sup> we published preliminary information regarding the reaction of  $[N(PPh_3)_2][Ru_3(CO)_9(B_2H_5)]$  with  $[Ru_3(CO)_{10}(NCMe)_2]$ . Significantly, this reaction gives *both* the octahedral boride cluster  $[Ru_6(CO)_{17}B]^-$  **1**<sup>13,19</sup> and the trigonal-prismatic cluster  $[Ru_6H_2(CO)_{18}B]^-$  **2**. We now present a full report of this work, and describe reactions of anions **1** and **2** with the gold(I) phosphines  $[AuCl(PR_3)]$  and  $\{[(R_3P)Au]_3O\}[BF_4]$  (R = Ph or 2-MeC<sub>6</sub>H<sub>4</sub>), all of which lead to hexaruthenium boride derivatives with octahedral cluster cores.

## Experimental

**General Data.**—Fourier-transform NMR spectra were recorded on a Bruker WM 250 or AM 400 spectrometer; <sup>1</sup>H shifts are reported with respect to δ 0 for SiMe<sub>4</sub>, <sup>11</sup>B with respect to δ 0 for F<sub>3</sub>B-OEt<sub>2</sub> and <sup>31</sup>P with respect to δ 0 for H<sub>3</sub>PO<sub>4</sub>. All spectral data listed in the Experimental section are recorded at 298 K. All downfield chemical shifts are positive. Infrared spectra were recorded on a Perkin Elmer FT 1710 spectrophotometer, FAB (fast atom bombardment) and FIB (fast ion bombardment) mass spectra on Kratos instruments with 3-nitrobenzyl alcohol as matrix.

† Supplementary data available: see Instructions for Authors, *J. Chem. Soc., Dalton Trans.*, 1993, Issue 1, pp. xxiii–xxviii.

Non-SI unit employed: atm = 101 325 Pa.



All reactions were carried out under argon by using standard Schlenk techniques. Solvents were dried over suitable reagents and freshly distilled under N<sub>2</sub> before use. Separations were carried out by thin-layer plate chromatography with Kieselgel 60-PF-254 (Merck). The compounds  $[AuCl(PPh_3)]$ ,  $[AuCl\{P(C_6H_4Me-2)_3\}]$ ,  $\{[(Ph_3P)Au]_3O\}[BF_4]$  and  $\{[(2-MeC_6H_4)_3PAu]_3O\}[BF_4]$  were made by published methods.<sup>20,21</sup> PPh<sub>3</sub> and P(C<sub>6</sub>H<sub>4</sub>Me-2)<sub>3</sub> were used as received (Aldrich) and  $[Ru_3(CO)_{10}(NCMe)_2]$  was prepared by the literature route.<sup>22</sup> Yields given are those obtained for a typical reaction.

**Preparation of  $[N(PPh_3)_2][Ru_3(CO)_9(B_2H_5)]$ .**—In a typical reaction  $[N(PPh_3)_2]Cl$  (74 mg, 0.13 mmol) and Na<sub>2</sub>CO<sub>3</sub> (14 mg, 0.13 mmol) were dissolved in methanol (5 cm<sup>3</sup>). In a separate flask,  $[Ru_3H(CO)_9(B_2H_5)]$  (prepared as previously reported)<sup>23</sup> (50 mg, 0.08 mmol) was dissolved in CH<sub>2</sub>Cl<sub>2</sub> (10 cm<sup>3</sup>). The latter solution was added to the former dropwise over a period of approximately 5 min. The solution was stirred

for 15 min and then the solvent was removed *in vacuo*. Unreacted neutral  $[\text{Ru}_3\text{H}(\text{CO})_9(\text{B}_2\text{H}_5)]$  was extracted into hexane; subsequent extraction with  $\text{Et}_2\text{O}$  removed solid sodium carbonate and excess of  $[\text{N}(\text{PPh}_3)_2]\text{Cl}$ . The salt  $[\text{N}(\text{PPh}_3)_2]\text{[Ru}_3(\text{CO})_9(\text{B}_2\text{H}_5)]^{24}$  can be produced in yields of > 80% with respect to its conjugate acid by this method: 400 MHz  $^1\text{H}$  NMR ( $\text{CD}_2\text{Cl}_2$ ,  $\delta$  7.6–7.5 (m, Ph in cation), +4.5 (br, 2 H, terminal BH), –0.4 (br, 1 H, B–H–B) and –12.8 (br, 2 H, Ru–H–B); 128 MHz  $^{11}\text{B}$  NMR ( $\text{CD}_2\text{Cl}_2$ ),  $\delta$  +18.4; IR ( $\text{CH}_2\text{Cl}_2$ ,  $\text{cm}^{-1}$ )  $\nu_{\text{BH}}$  2338w, 2304w;  $\nu_{\text{CO}}$  2057m, 2005vs, 1978s and 1952m; FAB MS,  $m/z$  582 ( $P^-$ ) (calc. for  $^{12}\text{C}_9\text{H}_5\text{B}_2\text{O}_9\text{Ru}_3$ :  $m/z$  582) with seven CO losses.

**Preparation of  $[\text{N}(\text{PPh}_3)_2]\text{[Ru}_6(\text{CO})_{17}\text{B}]$  and  $[\text{N}(\text{PPh}_3)_2]\text{[Ru}_6\text{H}_2(\text{CO})_{18}\text{B}]$ .**—The compound  $[\text{Ru}_3(\text{CO})_{10}(\text{NCMe})_2]$  was prepared from  $[\text{Ru}_3(\text{CO})_{12}]^{22}$  (130 mg, 0.20 mmol) in  $\text{CH}_2\text{Cl}_2$  (60  $\text{cm}^3$ ) and MeCN (10  $\text{cm}^3$ ) and the solution was added, after filtration through silica, to a solution of  $[\text{N}(\text{PPh}_3)_2]\text{[Ru}_3(\text{CO})_9(\text{B}_2\text{H}_5)]$  (170 mg, 0.15 mmol) in  $\text{CH}_2\text{Cl}_2$  (10  $\text{cm}^3$ ). The reaction mixture was stirred for 1 h at room temperature, changing from orange to brown. Products were separated by TLC, eluting with  $\text{CH}_2\text{Cl}_2$ –hexane (1:1). The first (yellow) fraction to be collected was composed of a mixture of  $[\text{Ru}_3\text{H}(\text{CO})_9(\text{B}_2\text{H}_5)]^{23}$ ,  $[\text{Ru}_4\text{H}(\text{CO})_{12}(\text{BH}_2)]^{25,26}$ ,  $[\text{Ru}_4\text{H}_4\text{-(CO)}_{12}]^{27}$  and  $[\text{Ru}_4\text{H}_2(\text{CO})_{13}]^{27}$ . The third (orange,  $\approx$  20%) fraction was  $[\text{N}(\text{PPh}_3)_2]\text{[Ru}_6\text{H}_2(\text{CO})_{18}\text{B}]$ . The fourth fraction (dark brown) was a mixture of  $[\text{N}(\text{PPh}_3)_2]\text{[Ru}_6(\text{CO})_{17}\text{B}]^{13}$  and  $[\text{N}(\text{PPh}_3)_2]\text{[Ru}_7(\text{CO})_{20}\text{B}]$  3 (see text), in an approximate ratio of 2:1 implied by  $^{11}\text{B}$  NMR spectral integrals. The second band has eluded characterisation.  $[\text{N}(\text{PPh}_3)_2]\text{[Ru}_6\text{H}_2\text{-(CO)}_{18}\text{B}]$ : 400 MHz  $^1\text{H}$  NMR ( $\text{CD}_2\text{Cl}_2$ ),  $\delta$  7.7–7.5 (m, Ph) and –17.1 (s, Ru–H–Ru); 128 MHz  $^{11}\text{B}$  NMR ( $\text{CD}_2\text{Cl}_2$ ),  $\delta$  +205.9; IR ( $\text{CH}_2\text{Cl}_2$ ,  $\text{cm}^{-1}$ ) 2042vs, 2031s, 2011w and 1987m; FAB MS,  $m/z$  1123 ( $P^-$ ) (calc. for  $^{12}\text{C}_{18}\text{H}_2\text{B}_2\text{O}_{18}\text{Ru}_6$ :  $m/z$  1123) with nine CO losses.

**Reaction of  $[\text{N}(\text{PPh}_3)_2]\text{[Ru}_6(\text{CO})_{17}\text{B}]$  with  $[\text{AuCl}(\text{PPh}_3)]$ .**—In a typical reaction,  $[\text{AuCl}(\text{PPh}_3)]$  (30 mg, 0.06 mmol) and TIPF<sub>6</sub> (4 mg, 0.01 mmol) were added to  $[\text{N}(\text{PPh}_3)_2]\text{[Ru}_6\text{-(CO)}_{17}\text{B}]$  (35 mg, 0.02 mmol)\* in  $\text{CH}_2\text{Cl}_2$  (5  $\text{cm}^3$ ) and the reaction mixture was stirred for 1 h. Two products were separated by TLC, eluting with  $\text{CH}_2\text{Cl}_2$ –hexane (2:1). The first (orange) fraction was identified as  $[\text{Ru}_4\text{H}_3(\text{CO})_{12}\{\text{Au}(\text{PPh}_3)\}]^{28}$  ( $\approx$  20%). The second fraction (red-brown) was  $[\text{Ru}_6(\text{CO})_{17}\text{B}\{\text{Au}(\text{PPh}_3)\}]$  4 ( $\approx$  70%): 400 MHz  $^1\text{H}$  NMR ( $\text{CDCl}_3$ ),  $\delta$  7.6–7.4 (m, Ph); 128 MHz  $^{11}\text{B}$  NMR ( $\text{CDCl}_3$ ),  $\delta$  +194.4; 162 MHz  $^{31}\text{P}$  NMR ( $\text{CDCl}_3$ ),  $\delta$  +73.7; IR ( $\text{CH}_2\text{Cl}_2$ ,  $\text{cm}^{-1}$ ) 2086w, 2054vs, 2042s, 2038s, 2023m, 1994m, 1975w and 1824w; FAB MS,  $m/z$  1555 ( $P^+$ ) (calc. for  $^{12}\text{C}_{35}\text{H}_{15}\text{B}_2\text{O}_{17}\text{Au}^{11}\text{B}_2\text{O}_{17}\text{P}_2\text{Ru}_6$ :  $m/z$  1552) with 17 CO losses.

**Reaction of  $[\text{N}(\text{PPh}_3)_2]\text{[Ru}_6\text{H}_2(\text{CO})_{18}\text{B}]$  with  $[\text{AuCl}(\text{PPh}_3)]$ .**—In a typical reaction,  $[\text{AuCl}(\text{PPh}_3)]$  (30 mg, 0.06 mmol) and TIPF<sub>6</sub> (4 mg, 0.01 mmol) were added to  $[\text{N}(\text{PPh}_3)_2]\text{[Ru}_6\text{H}_2(\text{CO})_{18}\text{B}]$  (33 mg, 0.02 mmol) in  $\text{CH}_2\text{Cl}_2$  (5  $\text{cm}^3$ ) and the reaction mixture was stirred for 1 h. Products were separated by TLC, eluting with  $\text{CH}_2\text{Cl}_2$ –hexane (3:1). The first two fractions were weak and were discarded. The third fraction (red-brown) was  $[\text{Ru}_6(\text{CO})_{17}\text{B}\{\text{Au}(\text{PPh}_3)\}]$  4 ( $\approx$  20%), the fourth (orange) was  $[\text{Ru}_6\text{H}(\text{CO})_{16}\text{B}\{\text{Au}(\text{PPh}_3)\}_2]$  5 ( $\approx$  20%), and the fifth (red-brown) was  $[\text{Ru}_6(\text{CO})_{16}\text{B}\{\text{Au}(\text{PPh}_3)\}_3]$  6 ( $\approx$  30%). Compound 5: 400 MHz  $^1\text{H}$  NMR ( $\text{CDCl}_3$ ),  $\delta$  7.8–6.9

\* Although  $[\text{N}(\text{PPh}_3)_2]\text{[Ru}_6(\text{CO})_{17}\text{B}]$  and  $[\text{N}(\text{PPh}_3)_2]\text{[Ru}_7(\text{CO})_{20}\text{B}]$  could not be separated, it was possible to use the mixture as a suitable starting material for reactions with gold(I) phosphines since the gold(I) phosphine derivatives of 1 were readily separated by TLC. No derivatives of 3 were isolated. The relative amounts of the two salts present in a sample could be deduced from the  $^{11}\text{B}$  NMR spectral integrals; comparison of the integrals is valid as the environments about the boron nuclei are very similar in 1 and 3.

(m, Ph) and –14.47 (Ru–H–Ru); 128 MHz  $^{11}\text{B}$  NMR ( $\text{CDCl}_3$ ),  $\delta$  +193.4; 162 MHz  $^{31}\text{P}$  NMR ( $\text{CDCl}_3$ ),  $\delta$  +61.4; IR ( $\text{CH}_2\text{Cl}_2$ ,  $\text{cm}^{-1}$ ) 2072m, 2044vs, 2024s, 2004m, 1971w, 1952w and 1817w; FIB MS,  $m/z$  1984 ( $P^+$ ) (calc. for  $^{12}\text{C}_{52}\text{H}_{31}\text{B}_2\text{O}_{16}\text{Au}_2\text{Ru}_6$ :  $m/z$  1984) with three CO losses. Compound 6: 400 MHz  $^1\text{H}$  NMR ( $\text{CDCl}_3$ ),  $\delta$  7.8–7.1 (m, Ph); 128 MHz  $^{11}\text{B}$  NMR ( $\text{CDCl}_3$ ),  $\delta$  +194.2; 162 MHz  $^{31}\text{P}$  NMR ( $\text{CDCl}_3$ ),  $\delta$  +60.1 (2P) and +67.5 (1P); IR ( $\text{CH}_2\text{Cl}_2$ ,  $\text{cm}^{-1}$ ) 2056w, 2034s, 2006vs and 1952w; FIB MS,  $m/z$  2442 ( $P^+$ ) (calc. for  $^{12}\text{C}_{70}\text{H}_{45}\text{B}_2\text{O}_{16}\text{Au}_3\text{Ru}_6$ :  $m/z$  2442) with five CO losses.

**Reaction of  $[\text{N}(\text{PPh}_3)_2]\text{[Ru}_6(\text{CO})_{17}\text{B}]$  with  $[\text{AuCl}\{\text{P}(\text{C}_6\text{H}_4\text{Me}-2)_3\}]$ .**—In a typical reaction  $[\text{AuCl}\{\text{P}(\text{C}_6\text{H}_4\text{Me}-2)_3\}]$  (32 mg, 0.06 mmol) and TIPF<sub>6</sub> (4 mg, 0.01 mmol) were added to  $[\text{N}(\text{PPh}_3)_2]\text{[Ru}_6(\text{CO})_{17}\text{B}]$  (35 mg, 0.02 mmol) in  $\text{CH}_2\text{Cl}_2$  (5  $\text{cm}^3$ ) and the reaction mixture was stirred for 30 min. Two products were separated by TLC, eluting with  $\text{CH}_2\text{Cl}_2$ –hexane (2:1). The first (orange) fraction was identified as  $[\text{Ru}_4\text{H}_3\text{-(CO)}_{12}\{\text{AuP}(\text{C}_6\text{H}_4\text{Me}-2)_3\}]$  ( $\approx$  30%) from its IR,  $^1\text{H}$  NMR and mass spectral properties (see below) and by a comparison of the data with those of the phenyl analogue.<sup>28</sup> The second fraction (red-brown) was  $[\text{Ru}_6(\text{CO})_{17}\text{B}\{\text{AuP}(\text{C}_6\text{H}_4\text{Me}-2)_3\}]$  7 ( $\approx$  50%): 400 MHz  $^1\text{H}$  NMR ( $\text{CDCl}_3$ ),  $\delta$  7.7–7.3 (m, Ph) and 2.4 (s, Me); 128 MHz  $^{11}\text{B}$  NMR ( $\text{CDCl}_3$ ),  $\delta$  +194.5; 162 MHz  $^{31}\text{P}$  NMR ( $\text{CDCl}_3$ ),  $\delta$  +66.4; IR ( $\text{CH}_2\text{Cl}_2$ ,  $\text{cm}^{-1}$ ) 2085w, 2052vs, 2042s, 2037s, 2022m, 1994m, 1976w, 1871w and 1850w; FAB MS,  $m/z$  1594 ( $P^+$ ) (calc. for  $^{12}\text{C}_{38}\text{H}_{21}\text{B}_2\text{O}_{17}\text{Au}^{11}\text{B}_2\text{O}_{17}\text{P}_2\text{Ru}_6$ :  $m/z$  1594) with one CO loss and loss of  $\text{AuP}(\text{C}_6\text{H}_4\text{Me}-2)_3$ , molecular ion at  $m/z$  1093 is very intense.

**Reaction of  $[\text{N}(\text{PPh}_3)_2]\text{[Ru}_6\text{H}_2(\text{CO})_{18}\text{B}]$  with  $[\text{AuCl}\{\text{P}(\text{C}_6\text{H}_4\text{Me}-2)_3\}]$ .**—In a typical reaction,  $[\text{AuCl}\{\text{P}(\text{C}_6\text{H}_4\text{Me}-2)_3\}]$  (32 mg, 0.06 mmol) and TIPF<sub>6</sub> (5 mg, 0.01 mmol) were added to  $[\text{N}(\text{PPh}_3)_2]\text{[Ru}_6\text{H}_2(\text{CO})_{18}\text{B}]$  (33 mg, 0.02 mmol) in  $\text{CH}_2\text{Cl}_2$  (5  $\text{cm}^3$ ). The reaction mixture was stirred for 1 h at room temperature. The products were separated by TLC eluting with hexane– $\text{CH}_2\text{Cl}_2$  (2:1). The first two fractions were of very low yield and were discarded. The third fraction was  $[\text{Ru}_6(\text{CO})_{17}\text{B}\{\text{AuP}(\text{C}_6\text{H}_4\text{Me}-2)_3\}]$  7 ( $\approx$  10% yield) and the fourth (orange) was identified as  $[\text{Ru}_6\text{H}(\text{CO})_{16}\text{B}\{\text{AuP}(\text{C}_6\text{H}_4\text{Me}-2)_3\}_2]$  8 ( $\approx$  30%). The fifth fraction comprised unreacted  $[\text{N}(\text{PPh}_3)_2]\text{[Ru}_6\text{H}_2(\text{CO})_{18}\text{B}]$  (typically  $\leq$  30% of the original starting material). Compound 8: 400 MHz  $^1\text{H}$  NMR ( $\text{CDCl}_3$ ),  $\delta$  7.7–7.3 (m, Ph) 2.6 (s, Me) and –14.50 (Ru–H–Ru); 128 MHz  $^{11}\text{B}$  NMR ( $\text{CDCl}_3$ ),  $\delta$  +194.0; 162 MHz  $^{31}\text{P}$  NMR ( $\text{CDCl}_3$ ),  $\delta$  +54.0; IR ( $\text{CH}_2\text{Cl}_2$ ,  $\text{cm}^{-1}$ ) 2052 m(sh), 2039 vs, 2016vs, 2003s, 1964m and 1806w; FIB MS,  $m/z$  2068 ( $P^-$ ) (calc. for  $^{12}\text{C}_{58}\text{H}_{43}\text{B}_2\text{O}_{16}\text{Au}_2\text{Ru}_6$ :  $m/z$  2068) with loss of one and two  $\text{AuP}(\text{C}_6\text{H}_4\text{Me}-2)_3$  with an intense envelope at  $m/z$  1065 followed by eight CO losses.

**Reaction of  $[\text{N}(\text{PPh}_3)_2]\text{[Ru}_6(\text{CO})_{17}\text{B}]$  with  $\{(\text{Ph}_3\text{P})\text{Au}\}_3\text{O}\text{[BF}_4\text{]}$ .**—In a typical reaction,  $\{(\text{Ph}_3\text{P})\text{Au}\}_3\text{O}\text{[BF}_4\text{]}$  (60 mg, 0.04 mmol) was added to  $[\text{N}(\text{PPh}_3)_2]\text{[Ru}_6(\text{CO})_{17}\text{B}]$  (34 mg, 0.02 mmol) in  $\text{CH}_2\text{Cl}_2$  (5  $\text{cm}^3$ ) and the resulting solution was stirred for 1 h at room temperature. Products were separated by TLC eluting with  $\text{CH}_2\text{Cl}_2$ –hexane (1:3). Two fractions were obtained. The first to be eluted was orange 4 (30% yield) and the second was red-brown 6 ( $\geq$  65% yield). No starting material remained. This route proved to be the best method of preparing cluster 6.

**Reaction of  $[\text{N}(\text{PPh}_3)_2]\text{[Ru}_6\text{H}_2(\text{CO})_{18}\text{B}]$  with  $\{(\text{Ph}_3\text{P})\text{Au}\}_3\text{O}\text{[BF}_4\text{]}$ .**—In a typical reaction, solid  $\{(\text{Ph}_3\text{P})\text{Au}\}_3\text{O}\text{[BF}_4\text{]}$  (80 mg, 0.05 mmol) was added to a  $\text{CH}_2\text{Cl}_2$  solution of  $[\text{N}(\text{PPh}_3)_2]\text{[Ru}_6\text{H}_2(\text{CO})_{18}\text{B}]$  (33 mg, 0.02 mmol) and the reaction solution was stirred for 1 h. Products were separated by TLC eluting with hexane– $\text{CH}_2\text{Cl}_2$  (2:1) to give many weak fractions. Only one fraction was collected (as the fifth band in very low yield) and this was identified as compound 6 by IR spectroscopy (see above).

*Reaction of [N(PPh<sub>3</sub>)<sub>2</sub>][Ru<sub>6</sub>(CO)<sub>17</sub>B] with [{(2-MeC<sub>6</sub>H<sub>4</sub>)<sub>3</sub>-PAu}<sub>3</sub>O][BF<sub>4</sub>].*—In a typical reaction, [{(2-MeC<sub>6</sub>H<sub>4</sub>)<sub>3</sub>-PAu}<sub>3</sub>O][BF<sub>4</sub>] (96 mg, 0.06 mmol) was added to [N(PPh<sub>3</sub>)<sub>2</sub>][Ru<sub>6</sub>(CO)<sub>17</sub>B] (35 mg, 0.02 mmol) in CH<sub>2</sub>Cl<sub>2</sub> (5 cm<sup>3</sup>) and the resulting solution was stirred for 1 h at room temperature. Products were separated by TLC eluting with CH<sub>2</sub>Cl<sub>2</sub>–hexane (1:2). The first fraction to be eluted was [Ru<sub>4</sub>H<sub>3</sub>(CO)<sub>12</sub>{AuP(C<sub>6</sub>H<sub>4</sub>Me-2)<sub>3</sub>}] (see above).<sup>28</sup> The second fraction was compound 7 ( $\approx$ 35% yield). The third fraction (red) was identified as [Ru<sub>6</sub>(CO)<sub>16</sub>B{AuP(C<sub>6</sub>H<sub>4</sub>Me-2)<sub>3</sub>}]<sup>9</sup> ( $\approx$ 40% yield). This route was the only method of preparing 9. Compound 9: 400 MHz <sup>1</sup>H NMR (CDCl<sub>3</sub>),  $\delta$  7.7–7.3 (m, Ph) and 2.4 (s, Me); 128 MHz <sup>11</sup>B NMR (CDCl<sub>3</sub>),  $\delta$  +193.7; 162 MHz <sup>31</sup>P NMR (CDCl<sub>3</sub>),  $\delta$  +61.0 (1 P) and +58.4 (2 P); IR (CH<sub>2</sub>Cl<sub>2</sub>, cm<sup>-1</sup>) 2139w, 2034s, 2007vs and 1954m; FIB MS, *m/z* 2570 (P<sup>+</sup>) (calc. for <sup>12</sup>C<sub>79</sub><sup>1</sup>H<sub>6</sub><sub>3</sub><sup>197</sup>Au<sub>3</sub><sup>11</sup>B<sup>16</sup>O<sub>16</sub><sup>31</sup>P<sub>3</sub><sup>101</sup>Ru<sub>6</sub>: *m/z* 2568) with loss of three AuP(C<sub>6</sub>H<sub>4</sub>Me-2)<sub>3</sub> with an intense envelope at *m/z* 1065.

*Reaction of [N(PPh<sub>3</sub>)<sub>2</sub>][Ru<sub>6</sub>H<sub>2</sub>(CO)<sub>18</sub>B] with [{(2-MeC<sub>6</sub>H<sub>4</sub>)<sub>3</sub>-PAu}<sub>3</sub>O][BF<sub>4</sub>].*—In a typical reaction, [{(2-MeC<sub>6</sub>H<sub>4</sub>)<sub>3</sub>-PAu}<sub>3</sub>O][BF<sub>4</sub>] (96 mg, 0.06 mmol) was added to [N(PPh<sub>3</sub>)<sub>2</sub>][Ru<sub>6</sub>H<sub>2</sub>(CO)<sub>18</sub>B] (35 mg, 0.02 mmol) in CH<sub>2</sub>Cl<sub>2</sub> (5 cm<sup>3</sup>) and the resulting solution was stirred for 1 h at room temperature during which time it became more red in colour. Products were separated by TLC eluting with CH<sub>2</sub>Cl<sub>2</sub>–hexane (1:2); a total of fifteen bands were observed, and all but the first were too weak

to collect. The first fraction (orange) to be eluted was identified by IR spectroscopy as [Ru<sub>4</sub>H<sub>3</sub>(CO)<sub>12</sub>{AuP(C<sub>6</sub>H<sub>4</sub>Me-2)<sub>3</sub>}] (see above).<sup>28</sup>

*Reaction of [Ru<sub>6</sub>(CO)<sub>16</sub>B{Au(PPh<sub>3</sub>)<sub>3</sub>}]* with CO.—The compound [Ru<sub>6</sub>(CO)<sub>16</sub>B{Au(PPh<sub>3</sub>)<sub>3</sub>}]<sup>6</sup> (24 mg, 0.01 mmol) was dissolved in CH<sub>2</sub>Cl<sub>2</sub> (30 cm<sup>3</sup>) and heated at 50 °C under an atmosphere of CO (70 atm) for 2 d. Products were separated by TLC. The first fraction (blue) to be collected was [Ru<sub>5</sub>(CO)<sub>5</sub>B{Au(PPh<sub>3</sub>)<sub>3</sub>}]<sup>6</sup> ( $\approx$ 30%),<sup>29</sup> the second was the monogold derivative 4 ( $\approx$ 10%) and the final fraction was unreacted 5.

*Crystal Structure Determinations.*—Crystallographic data for [N(PPh<sub>3</sub>)<sub>2</sub>][Ru<sub>6</sub>H<sub>2</sub>(CO)<sub>18</sub>B] and 5–7 are in Table 1. Crystals were encapsulated in capillary tubes with epoxy resin and were photographically characterised. Compounds [N(PPh<sub>3</sub>)<sub>2</sub>][Ru<sub>6</sub>H<sub>2</sub>(CO)<sub>18</sub>B], 5 and 7 were found to have no symmetry higher than triclinic, whereas 6 was found to have 2/m Laue symmetry. The three triclinic crystals were initially assumed to be centrosymmetric; the results of refinement supported these assignments. Systematic absences in the diffraction data allowed a unique space-group assignment for the monoclinic cell. All data sets were corrected for absorption; corrections for [N(PPh<sub>3</sub>)<sub>2</sub>][Ru<sub>6</sub>H<sub>2</sub>(CO)<sub>18</sub>B], 5 and 7 used semiempirical  $\psi$ -scan methods, and 6 used XABS<sup>30a</sup> which obtains an empirical absorption tensor from an expression relating  $F_o$  and  $F_c$ .

All structures were solved by direct methods which in each

Table 1 Crystallographic data for [N(PPh<sub>3</sub>)<sub>2</sub>][Ru<sub>6</sub>H<sub>2</sub>(CO)<sub>18</sub>B] and 5–7

	[N(PPh <sub>3</sub> ) <sub>2</sub> ]-[Ru <sub>6</sub> H <sub>2</sub> (CO) <sub>18</sub> B]	5	6	7
<i>(a)</i> Crystal parameters				
Formula	C <sub>54</sub> H <sub>32</sub> BNO <sub>18</sub> P <sub>2</sub> Ru <sub>6</sub>	C <sub>52</sub> H <sub>31</sub> Au <sub>2</sub> BO <sub>16</sub> P <sub>2</sub> Ru <sub>6</sub>	C <sub>70</sub> H <sub>45</sub> Au <sub>3</sub> BO <sub>16</sub> P <sub>3</sub> Ru <sub>6</sub>	C <sub>38</sub> H <sub>21</sub> AuBO <sub>17</sub> PRu <sub>6</sub>
Formula weight	1661.98	1984.9	2443.1	1594.7
Crystal system	Triclinic	Triclinic	Monoclinic	Triclinic
Space group	<i>P</i> ī	<i>P</i> ī	<i>P</i> 2 <sub>1</sub> /c	<i>P</i> ī
<i>a</i> / $\text{\AA}$	13.459(1)	12.769(3)	19.894(4)	9.946(3)
<i>b</i> / $\text{\AA}$	15.417(2)	13.694(3)	18.251(4)	14.167(4)
<i>c</i> / $\text{\AA}$	15.432(2)	20.470(4)	22.624(5)	16.773(4)
$\alpha/^\circ$	109.42(1)	83.75(3)	—	79.70(2)
$\beta/^\circ$	94.86(1)	73.75(3)	98.00(3)	88.23(2)
$\gamma/^\circ$	102.81(1)	67.76(3)	—	74.19(2)
<i>U</i> / $\text{\AA}^3$	2900.8(9)	3180.7(12)	8135(4)	2236(2)
<i>Z</i>	2	2	4	2
Crystal dimensions/mm	0.25 × 0.30 × 0.42	0.30 × 0.32 × 0.36	0.20 × 0.32 × 0.33	0.06 × 0.19 × 0.42
Crystal colour	Orange	Black	Deep red	Deep red
<i>D</i> <sub>c</sub> /g cm <sup>-3</sup>	1.903	2.072	1.995	2.368
$\mu(\text{Mo-K}\alpha)/\text{cm}^{-1}$	16.5	60.9	65.9	53.43
<i>T</i> /K	298	298	295	296
<i>T</i> (max.)/ <i>T</i> (min.)	0.794, 0.392	0.742, 0.464	0.915, 0.232	1.00, 0.31
<i>F</i> (000)	1612	1856	4576	1496
<i>(b)</i> Data collection				
2 <i>θ</i> scan range/°	4–52	4–45	4–45	4–52
Reflections collected	11 019	8577	10 921	9125
Independent reflections	10 064	8296	10 608	8806
Independent observed reflections [ $F_o \geq n\sigma(F_o)$ ]	6906 ( <i>n</i> = 4)	5882 ( <i>n</i> = 4)	6974 ( <i>n</i> = 4)	6326 ( <i>n</i> = 6)
Variation in standards (%)	< 2	< 2	< 1	< 2
<i>(c)</i> Refinement				
<i>R</i>	0.0447	0.0587	0.0717	0.0408
<i>R'</i>	0.0481	0.0814	0.0733	0.0503
$\Delta/\sigma(\text{max.})$	0.016	0.043	0.041	0.062
$\Delta(p)/e \text{\AA}^{-3}$	0.79	3.16	3.23	2.04
<i>N<sub>o</sub></i> / <i>N<sub>v</sub></i>	14.2	9.2	14.4	11.0
Goodness of fit	1.25	1.73	1.63	1.24
<i>g</i> In weighting scheme, <i>w</i> <sup>-1</sup> = $\sigma^2(F) + gF^2$	0.0008	0.0010	0.0020	0.0008

\* Details in common: Siemens P4 diffractometer, graphite monochromator; Mo-K $\alpha$  radiation ( $\lambda$  = 0.710 73 Å); three standard reflections per 197.

case located the metal atoms. The refinements minimised  $F^2$  for  $[\text{N}(\text{PPh}_3)_2][\text{Ru}_6\text{H}_2(\text{CO})_{18}\text{B}]$ , **5** and **7**, and  $F$  for **6**, which accounts for its higher comparative  $R$  indices. All non-hydrogen atoms were anisotropically refined except the carbon atoms in the cation  $[\text{N}(\text{PPh}_3)_2]^+$  and the boron atom in **6** (which was persistently non-positive definite). The phenyl rings in  $[\text{N}(\text{PPh}_3)_2][\text{Ru}_6\text{H}_2(\text{CO})_{18}\text{B}]$ , **5** and **6** were constrained as rigid hexagons. All hydrogen atoms were idealised except for the two hydride ligands in  $[\text{N}(\text{PPh}_3)_2][\text{Ru}_6\text{H}_2(\text{CO})_{18}\text{B}]$ , which were located and refined with a common and constrained Ru-H distance of 1.75(1) Å, and the hydride in **5** which was ignored.

All computations used the SHELXTL-PLUS V4.2 software.<sup>30b</sup> Atomic coordinates are given in Tables 2, 4, 6 and 8 for  $[\text{N}(\text{PPh}_3)_2][\text{Ru}_6\text{H}_2(\text{CO})_{18}\text{B}]$ , **7**, **5** and **6**, respectively.

Additional material available from the Cambridge Crystallographic Data Centre comprises H-atom coordinates, thermal parameters and remaining bond lengths and angles.

## Results and Discussion

**Preparation of Compounds 1 and 2.**—The hexaruthenium boride anion  $[\text{Ru}_6(\text{CO})_{17}\text{B}]^-$  **1** was first reported by Shore and co-workers<sup>13</sup> and by us.<sup>19</sup> We have observed that the neutral boride  $[\text{Ru}_6\text{H}(\text{CO})_{17}\text{B}]$ <sup>13,14</sup> is formed spontaneously during the photolysis of  $[\text{Ru}_3(\text{CO})_9(\text{BH}_5)]$  with loss of  $\text{H}_2$  (and CO) presumably being the driving force for the reaction.<sup>14</sup> Following from this, we considered that a rational method of preparing anion **1** would be the reaction of  $[\text{Ru}_3(\text{CO})_9(\text{BH}_4)]^-$ <sup>14</sup> with  $[\text{Ru}_3(\text{CO})_{10}(\text{NCMe})_2]$ . In fact this reaction gave poor results, but the reaction of  $[\text{N}(\text{PPh}_3)_2][\text{Ru}_3(\text{CO})_9(\text{B}_2\text{H}_5)]$  with  $[\text{Ru}_3(\text{CO})_{10}(\text{NCMe})_2]$  produced  $[\text{N}(\text{PPh}_3)_2][\text{Ru}_6(\text{CO})_{17}\text{B}]$  in about 10% yield in addition to  $[\text{N}(\text{PPh}_3)_2][\text{Ru}_6\text{H}_2(\text{CO})_{18}\text{B}]$ , and a third product,  $[\text{N}(\text{PPh}_3)_2][\text{Ru}_7(\text{CO})_{20}\text{B}]$  **3** (see below). Anion **2** was confirmed by X-ray crystallography (see below) to exhibit a trigonal-prismatic  $\text{Ru}_6$ -cluster core. It is noteworthy that both octahedral, **1**, and trigonal-prismatic, **2**, boride clusters have been isolated. Perhaps even more significant is the fact that **1** and **2** are produced in the same reaction. The result indicates that the choice of the trigonal-prismatic *versus* octahedral cage is not determined by the size of the interstitial atom since in this case the latter is a common feature of **1** and **2**. Interestingly, the trigonal prism is a common building block for bulk metal-rich borides containing isolated boron atoms including ruthenium borides (*e.g.*  $\text{Ru}_7\text{B}_3$ ).<sup>31,32</sup>

The third product,  $[\text{N}(\text{PPh}_3)_2][\text{Ru}_7(\text{CO})_{20}\text{B}]$ , could not be purified. Upon repeated chromatographic separation of this mixture, a single fraction comprising two boron-containing products in a consistent ratio (by  $^{11}\text{B}$  NMR spectral analysis) of  $\approx 2:1$  persisted. The  $^{11}\text{B}$  NMR spectrum of this fraction dissolved in  $\text{CD}_2\text{Cl}_2$  showed two resonances at  $\delta + 198.8$  and  $+195.7$ . The former signal is due to the octahedral boride anion **1**; both low-field shifts are characteristic of an interstitial boron atom, and more significantly, one which is in contact with six ruthenium atoms.<sup>18,33</sup> Fast atom bombardment mass-spectral analysis of the fraction showed two well resolved envelopes at  $m/z$  1093 and 1278, each with sequential CO loss. The former is due to the parent ion of **1** and the latter is consistent with a formulation of  $[\text{Ru}_7(\text{CO})_{20}\text{B}]$  for **3** (calc. for  $^{12}\text{C}_{20}^{11}\text{B}^{16}\text{O}_{20}^{101}\text{Ru}_7$ :  $m/z$  1278). No  $^1\text{H}$  NMR resonances, other than those due to the  $[\text{N}(\text{PPh}_3)_2]^+$  cation, were observed for the mixture. These data allow us to propose the formulation  $[\text{N}(\text{PPh}_3)_2][\text{Ru}_7(\text{CO})_{20}\text{B}]$ . The anion  $[\text{Ru}_7(\text{CO})_{20}\text{B}]^-$  possesses 100 valence electrons and this count is consistent with an edge-bridged octahedral  $\text{Ru}_7$ -cage structure. We propose this structure, with the boron atom occupying the octahedral cavity.

**Molecular Structure of  $[\text{N}(\text{PPh}_3)_2][\text{Ru}_6\text{H}_2(\text{CO})_{18}\text{B}]$ .**—A crystal of this compound suitable for X-ray diffraction analysis was grown from  $\text{CH}_2\text{Cl}_2$  layered with hexane. The molecular structure of the anion **2** is shown in Fig. 1; atomic coordinates

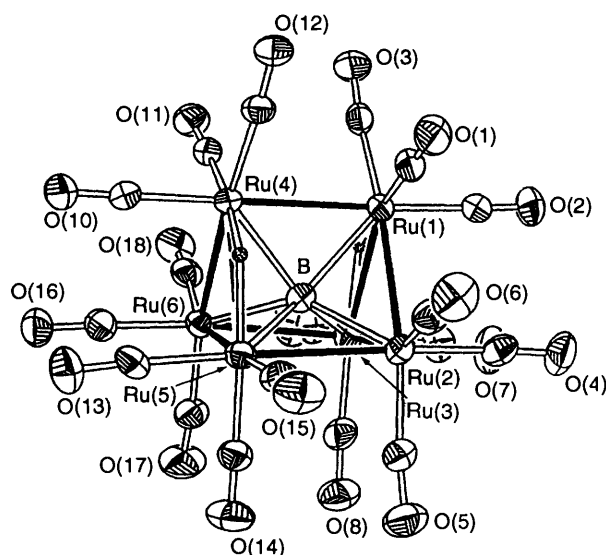


Fig. 1 Molecular structure of the anion  $[\text{Ru}_6\text{H}_2(\text{CO})_{18}\text{B}]^-$  **2**

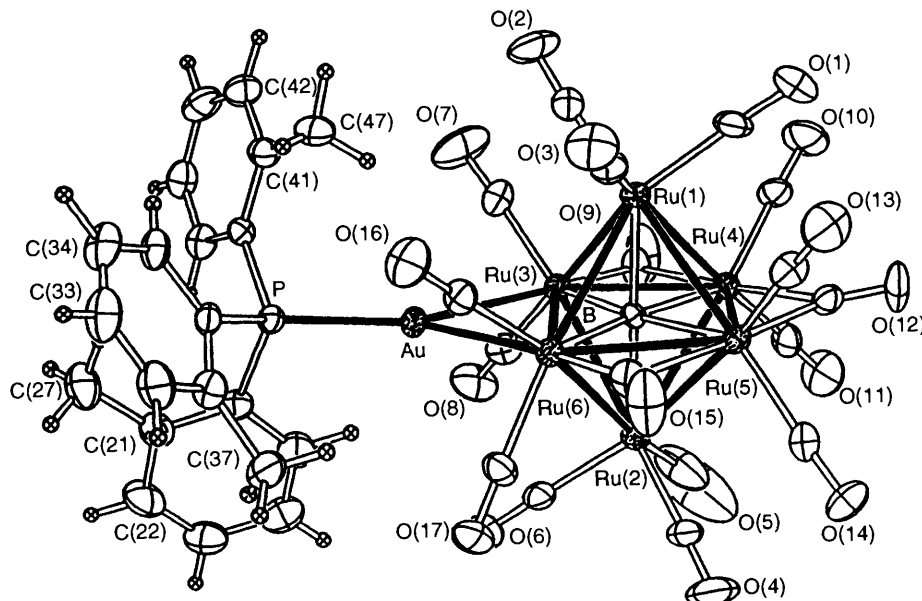
are given in Table 2 and selected bond distances and angles in Table 3. The six ruthenium atoms define a trigonal-prismatic cage and the boron atom resides at its centre. The metal framework is regular with  $\text{Ru}-\text{Ru}-\text{Ru}$   $90 \pm 2^\circ$  for the square faces and  $60 \pm 2^\circ$  for the triangular faces. The  $\text{Ru}-\text{B}$  distances are in the range 2.171–2.268 Å, longer than in the two isomers of the octahedral boride  $[\text{Ru}_6\text{H}(\text{CO})_{17}\text{B}]$ .<sup>13,14</sup> {The structure of  $[\text{Ru}_6(\text{CO})_{17}\text{B}]^-$  has not been reported.} There are no significant differences between the lengths of the  $\text{Ru}-\text{Ru}$  edges that define the triangular ends of the prism and the edges that define the prism height. Two hydride ligands have been located directly; each bridges one  $\text{Ru}-\text{Ru}$  edge of a different triangular face of the  $\text{Ru}_6$  prism, *viz.* edges  $\text{Ru}(1)-\text{Ru}(3)$  and  $\text{Ru}(4)-\text{Ru}(5)$ . The formulation of **2** is consistent with the 90-valence-electron count expected for a trigonal-prismatic transition-metal cluster.

**Reaction of  $[\text{Ru}_6(\text{CO})_{17}\text{B}]^-$  with  $[\text{AuCl}(\text{PR}_3)]$  (R = Ph or 2-MeC<sub>6</sub>H<sub>4</sub>).**—The salt  $[\text{N}(\text{PPh}_3)_2][\text{Ru}_6(\text{CO})_{17}\text{B}]$  reacts with  $[\text{AuCl}(\text{PPh}_3)]$  in the presence of TIPF<sub>6</sub> to give  $[\text{Ru}_4\text{H}_3(\text{CO})_{12}\{\text{Au}(\text{PPh}_3)\}]$ <sup>28</sup> and  $[\text{Ru}_6(\text{CO})_{17}\text{B}\{\text{Au}(\text{PPh}_3)\}]$  **4**. Compound **4** is characterised in solution by an  $^{11}\text{B}$  NMR spectral resonance at  $\delta + 194.4$  which is close to that of the starting material ( $\delta + 198.8$ ). This implies that the immediate environment of the boron nucleus has not been greatly perturbed. The reaction with  $[\text{AuCl}\{\text{P}(\text{C}_6\text{H}_4\text{Me}-2)_3\}]$  proceeds in a similar manner to give  $[\text{Ru}_6(\text{CO})_{17}\text{B}\{\text{AuP}(\text{C}_6\text{H}_4\text{Me}-2)_3\}]$  **7**. Like **4**, compound **7** exhibits an  $^{11}\text{B}$  NMR spectral signal ( $\delta + 194.5$ ) close to that of **1**. Both **4** and **7** exhibit virtually identical solution infrared spectra, indicating that their structures are similar. We would anticipate that the structures would be related to that of the neutral  $[\text{Ru}_6\text{H}(\text{CO})_{17}\text{B}]$ <sup>13,14</sup> by the replacement of the edge-bridging hydride ligand by an isolobal  $\{\text{R}_3\text{PAu}\}$  fragment. However, examples<sup>34</sup> illustrate that a gold(i) unit associated with a transition-metal cluster of nuclearity four or more may prefer to cap a trimetal face rather than bridge a dimetal edge. Thus we undertook an X-ray diffraction study of **7**.

**Molecular Structure of  $[\text{Ru}_6(\text{CO})_{17}\text{B}\{\text{AuP}(\text{C}_6\text{H}_4\text{Me}-2)_3\}]$  **7**.**—An X-ray-quality crystal of compound **7** was grown from  $\text{CH}_2\text{Cl}_2$  layered with ethanol. The molecular structure is shown in Fig. 2; atomic coordinates are given in Table 4 and selected bond distances and angles in Table 5. The  $\text{Ru}_6$  cage possesses an octahedral geometry as expected for an 86-electron cluster. The boron atom resides centrally with  $\text{Ru}-\text{B}$  distances ranging from 2.07 to 2.14 Å. Atoms  $\text{Ru}(1)$  and  $\text{Ru}(2)$  each carry three terminal

**Table 2** Atomic coordinates ( $\times 10^4$ ) for  $[\text{N}(\text{PPh}_3)_2]\text{[Ru}_6\text{H}_2(\text{CO})_{18}\text{B}]$ 

Atom	<i>x</i>	<i>y</i>	<i>z</i>	Atom	<i>x</i>	<i>y</i>	<i>z</i>
Ru(1)	4 647(1)	7 903(1)	322(1)	C(14)	4 538(6)	8 757(6)	3 965(6)
Ru(2)	5 552(1)	9 259(1)	2 133(1)	C(15)	3 698(6)	10 032(6)	3 278(5)
Ru(3)	5 765(1)	7 363(1)	1 686(1)	C(16)	2 558(7)	6 413(6)	2 711(6)
Ru(4)	2 717(1)	7 392(1)	993(1)	C(17)	4 583(7)	6 657(6)	3 253(6)
Ru(5)	3 686(1)	8 706(1)	2 891(1)	C(18)	3 625(7)	5 510(6)	1 395(6)
Ru(6)	3 768(1)	6 763(1)	2 244(1)	C(31)	3 161(1)	3 375(1)	3 855(1)
P(1)	1 323(2)	2 748(1)	2 598(1)	C(32)	4 225	3 768	4 145
P(2)	138(2)	2 641(2)	4 137(1)	C(33)	4 827	4 071	3 555
B	4 381(6)	7 912(6)	1 742(6)	C(34)	4 365	3 983	2 675
N	735(5)	3 019(5)	3 454(5)	C(35)	3 300	3 590	2 385
O(1)	3 862(5)	9 470(5)	-39(5)	C(36)	2 698	3 286	2 975
O(2)	6 604(5)	8 383(5)	-485(5)	C(41)	1 942(1)	1 073(1)	1 938(1)
O(3)	3 550(5)	6 445(5)	-1 572(4)	C(42)	1 750	89	1 491
O(4)	7 539(5)	9 969(5)	1 469(5)	C(43)	742	-468	1 091
O(5)	6 636(5)	10 315(5)	4 137(4)	C(44)	-73	-41	1 138
O(6)	4 802(5)	10 905(4)	1 912(5)	C(45)	119	944	1 585
O(7)	7 857(5)	7 923(6)	1 118(6)	C(46)	1 126	1 501	1 985
O(8)	6 860(5)	8 105(6)	3 703(5)	C(51)	421(1)	3 971(1)	2 057(1)
O(9)	5 866(6)	5 305(5)	1 224(6)	C(52)	148	4 395	1 435
O(10)	695(5)	6 961(6)	1 701(4)	C(53)	341	4 071	524
O(11)	2 251(5)	5 365(4)	-378(4)	C(54)	806	3 323	235
O(12)	1 748(4)	7 969(5)	-508(4)	C(55)	1 079	2 899	856
O(13)	1 814(5)	8 255(5)	3 790(5)	C(56)	887	3 223	1 768
O(14)	5 012(5)	8 821(5)	4 629(4)	C(61)	1 281(1)	4 331(1)	5 515(1)
O(15)	3 673(5)	10 795(4)	3 538(4)	C(62)	1 771	4 904	6 424
O(16)	1 837(5)	6 159(5)	3 013(4)	C(63)	1 717	4 531	7 133
O(17)	5 005(6)	6 535(6)	3 832(5)	C(64)	1 174	3 584	6 932
O(18)	3 498(5)	4 736(5)	911(5)	C(65)	684	3 012	6 022
C(1)	4 140(6)	8 886(6)	125(6)	C(66)	738	3 385	5 313
C(2)	5 895(6)	8 227(6)	-172(6)	C(71)	1 040(1)	1 218(1)	4 185(1)
C(3)	3 936(6)	6 962(6)	-846(6)	C(72)	1 047	275	4 027
C(4)	6 790(6)	9 661(6)	1 693(6)	C(73)	123	-447	3 704
C(5)	6 201(6)	9 889(6)	3 401(6)	C(74)	-808	-225	3 538
C(6)	5 051(7)	10 265(6)	1 990(6)	C(75)	-815	718	3 696
C(7)	7 063(7)	7 717(7)	1 319(7)	C(76)	109	1 440	4 019
C(8)	6 407(6)	7 821(7)	2 948(7)	C(81)	-1 713(1)	2 924(1)	4 724(1)
C(9)	5 803(7)	6 050(6)	1 377(7)	C(82)	-2 765	2 865	4 557
C(10)	1 458(6)	7 112(6)	1 434(6)	C(83)	-3 283	2 583	3 645
C(11)	2 488(6)	6 130(6)	144(5)	C(84)	-2 747	2 361	2 900
C(12)	2 133(6)	7 796(6)	69(5)	C(85)	-1 695	2 421	3 067
C(13)	2 498(6)	8 402(6)	3 431(5)	C(86)	-1 178	2 703	3 979

**Fig. 2** Molecular structure of  $[\text{Ru}_6(\text{CO})_{17}\text{B}\{\text{AuP}(\text{C}_6\text{H}_4\text{Me}-2)\}_3]$  7

carbonyl ligands, and these two  $\text{Ru}(\text{CO})_3$  units are mutually staggered. Each of the remaining four ruthenium atoms bears

**Table 3** Selected bond distances ( $\text{\AA}$ ) and angles ( $^\circ$ ) for anion **2**

$\text{Ru}(1)\text{-Ru}(2)$	2.841(1)	$\text{Ru}(1)\text{-Ru}(3)$	2.929(1)
$\text{Ru}(1)\text{-Ru}(4)$	2.921(1)	$\text{Ru}(1)\text{-B}$	2.247(10)
$\text{Ru}(2)\text{-Ru}(3)$	2.858(1)	$\text{Ru}(2)\text{-Ru}(5)$	2.935(1)
$\text{Ru}(2)\text{-B}$	2.171(8)	$\text{Ru}(3)\text{-Ru}(6)$	2.939(1)
$\text{Ru}(3)\text{-B}$	2.208(9)	$\text{Ru}(4)\text{-Ru}(5)$	2.936(1)
$\text{Ru}(4)\text{-Ru}(6)$	2.838(1)	$\text{Ru}(4)\text{-B}$	2.268(8)
$\text{Ru}(5)\text{-Ru}(6)$	2.856(1)	$\text{Ru}(5)\text{-B}$	2.204(9)
$\text{Ru}(6)\text{-B}$	2.188(10)		
$\text{Ru}(2)\text{-Ru}(1)\text{-Ru}(3)$	59.3(1)	$\text{Ru}(2)\text{-Ru}(1)\text{-Ru}(4)$	89.9(1)
$\text{Ru}(3)\text{-Ru}(1)\text{-Ru}(4)$	90.8(1)	$\text{Ru}(2)\text{-Ru}(1)\text{-B}$	48.8(2)
$\text{Ru}(3)\text{-Ru}(1)\text{-B}$	48.3(2)	$\text{Ru}(4)\text{-Ru}(1)\text{-B}$	50.0(2)
$\text{Ru}(1)\text{-Ru}(2)\text{-Ru}(3)$	61.9(1)	$\text{Ru}(1)\text{-Ru}(2)\text{-Ru}(5)$	91.9(1)
$\text{Ru}(3)\text{-Ru}(2)\text{-Ru}(5)$	88.9(1)	$\text{Ru}(1)\text{-Ru}(2)\text{-B}$	51.2(2)
$\text{Ru}(3)\text{-Ru}(2)\text{-B}$	49.8(3)	$\text{Ru}(5)\text{-Ru}(2)\text{-B}$	48.4(2)
$\text{Ru}(1)\text{-Ru}(3)\text{-Ru}(2)$	58.8(1)	$\text{Ru}(1)\text{-Ru}(3)\text{-Ru}(6)$	87.4(1)
$\text{Ru}(2)\text{-Ru}(3)\text{-Ru}(6)$	90.7(1)	$\text{Ru}(1)\text{-Ru}(3)\text{-B}$	49.5(3)
$\text{Ru}(2)\text{-Ru}(3)\text{-B}$	48.7(2)	$\text{Ru}(6)\text{-Ru}(3)\text{-B}$	47.8(3)
$\text{Ru}(1)\text{-Ru}(4)\text{-Ru}(5)$	90.3(1)	$\text{Ru}(1)\text{-Ru}(4)\text{-Ru}(6)$	89.4(1)
$\text{Ru}(5)\text{-Ru}(4)\text{-Ru}(6)$	59.3(1)	$\text{Ru}(1)\text{-Ru}(4)\text{-B}$	49.4(2)
$\text{Ru}(5)\text{-Ru}(4)\text{-B}$	48.0(2)	$\text{Ru}(6)\text{-Ru}(4)\text{-B}$	49.2(2)
$\text{Ru}(2)\text{-Ru}(5)\text{-Ru}(4)$	87.8(1)	$\text{Ru}(2)\text{-Ru}(5)\text{-Ru}(6)$	90.8(1)
$\text{Ru}(4)\text{-Ru}(5)\text{-Ru}(6)$	58.7(1)	$\text{Ru}(2)\text{-Ru}(5)\text{-B}$	47.4(2)
$\text{Ru}(4)\text{-Ru}(5)\text{-B}$	49.9(2)	$\text{Ru}(6)\text{-Ru}(5)\text{-B}$	49.2(3)
$\text{Ru}(3)\text{-Ru}(6)\text{-Ru}(4)$	92.2(1)	$\text{Ru}(3)\text{-Ru}(6)\text{-Ru}(5)$	88.9(1)
$\text{Ru}(4)\text{-Ru}(6)\text{-Ru}(5)$	62.1(1)	$\text{Ru}(3)\text{-Ru}(6)\text{-B}$	48.3(2)
$\text{Ru}(4)\text{-Ru}(6)\text{-B}$	51.7(2)	$\text{Ru}(5)\text{-Ru}(6)\text{-B}$	49.7(2)
$\text{Ru}(1)\text{-B}\text{-Ru}(2)$	80.0(3)	$\text{Ru}(1)\text{-B}\text{-Ru}(3)$	82.2(3)
$\text{Ru}(2)\text{-B}\text{-Ru}(3)$	81.5(3)	$\text{Ru}(1)\text{-B}\text{-Ru}(4)$	80.6(3)
$\text{Ru}(2)\text{-B}\text{-Ru}(4)$	132.9(5)	$\text{Ru}(3)\text{-B}\text{-Ru}(4)$	137.1(4)
$\text{Ru}(1)\text{-B}\text{-Ru}(5)$	137.7(5)	$\text{Ru}(2)\text{-B}\text{-Ru}(5)$	84.2(3)
$\text{Ru}(3)\text{-B}\text{-Ru}(5)$	133.7(4)	$\text{Ru}(4)\text{-B}\text{-Ru}(5)$	82.1(3)
$\text{Ru}(1)\text{-B}\text{-Ru}(6)$	132.0(3)	$\text{Ru}(2)\text{-B}\text{-Ru}(6)$	142.2(4)
$\text{Ru}(3)\text{-B}\text{-Ru}(6)$	83.9(4)	$\text{Ru}(4)\text{-B}\text{-Ru}(6)$	79.1(3)
$\text{Ru}(5)\text{-B}\text{-Ru}(6)$	81.1(3)		

**Table 4** Atomic coordinates ( $\times 10^4$ ) for compound **7**

Atom	<i>x</i>	<i>y</i>	<i>z</i>	Atom	<i>x</i>	<i>y</i>	<i>z</i>
Au	2 179.9(4)	8 286.5(3)	7 685.3(2)	C(7)	4 825(10)	8 671(7)	6 776(6)
Ru(1)	2 162.0(7)	10 936.0(5)	6 083.5(4)	C(8)	4 737(9)	8 651(8)	8 411(6)
Ru(2)	2 235.3(8)	10 788.8(6)	8 571.0(4)	C(9)	5 490(10)	10 172(7)	7 449(7)
Ru(3)	3 895.2(7)	9 565.6(5)	7 474.2(4)	C(10)	4 925(10)	12 020(8)	6 360(6)
Ru(4)	3 804.9(7)	11 618.8(5)	7 209.1(4)	C(11)	4 730(11)	12 162(8)	7 900(6)
Ru(5)	825.5(7)	12 282.2(5)	7 143.1(4)	C(12)	2 319(10)	13 054(7)	6 925(6)
Ru(6)	508.9(7)	10 267.1(5)	7 450.3(4)	C(13)	-151(10)	13 053(7)	6 197(6)
P	2 200(2)	6 614(2)	7 855(1)	C(14)	-269(9)	13 203(7)	7 785(6)
B	2 227(9)	10 833(7)	7 326(5)	C(15)	-1 021(10)	11 471(8)	7 254(6)
O(1)	2 683(10)	12 692(7)	4 904(4)	C(16)	-312(9)	9 532(7)	6 829(6)
O(2)	3 712(10)	9 498(7)	5 007(5)	C(17)	-383(10)	9 856(8)	8 429(6)
O(3)	-567(8)	11 104(7)	5 225(5)	C(21)	2 345(11)	5 053(8)	9 236(6)
O(4)	40(14)	12 068(7)	9 499(5)	C(22)	2 633(14)	4 686(10)	10 069(7)
O(5)	4 535(17)	11 027(15)	9 578(7)	C(23)	3 107(13)	5 226(11)	10 538(7)
O(6)	2 300(10)	8 923(6)	9 794(5)	C(24)	3 355(13)	6 128(10)	10 223(7)
O(7)	5 407(10)	8 109(8)	6 394(6)	C(25)	3 077(12)	6 474(9)	9 421(6)
O(8)	5 276(9)	8 106(7)	8 955(4)	C(26)	2 569(9)	5 980(7)	8 905(5)
O(9)	6 668(7)	10 013(6)	7 519(7)	C(27)	1 825(13)	4 430(9)	8 752(7)
O(10)	5 576(9)	12 298(7)	5 858(5)	C(31)	-699(9)	6 832(7)	7 980(6)
O(11)	5 262(10)	12 510(8)	8 322(5)	C(32)	-1 946(11)	6 704(9)	7 709(7)
O(12)	2 415(8)	13 839(5)	6 714(6)	C(33)	-1 993(12)	6 247(8)	7 086(8)
O(13)	-738(9)	13 544(6)	5 640(5)	C(34)	-815(12)	5 876(9)	6 682(7)
O(14)	-966(8)	13 762(6)	8 118(5)	C(35)	439(10)	5 982(7)	6 907(6)
O(15)	-2 197(7)	11 903(6)	7 181(6)	C(36)	540(10)	6 456(7)	7 564(6)
O(16)	-835(8)	9 144(7)	6 455(5)	C(37)	-715(11)	7 364(9)	8 681(7)
O(17)	-969(9)	9 660(6)	8 983(5)	C(41)	3 604(10)	6 266(8)	6 402(5)
C(1)	2543(11)	12 002(8)	5 344(5)	C(42)	4 671(12)	5 732(9)	5 972(7)
C(2)	3 172(10)	9 989(7)	5 453(6)	C(43)	5 615(12)	4 892(10)	6 329(7)
C(3)	441(11)	11 038(8)	5 557(5)	C(44)	5 560(11)	4 555(8)	7 153(7)
C(4)	842(16)	11 616(9)	9 129(7)	C(45)	4 535(9)	5 073(8)	7 604(6)
C(5)	3 620(17)	11 035(14)	9 159(7)	C(46)	3 523(8)	5 925(6)	7 235(5)
C(6)	2 238(11)	9 613(8)	9 319(5)	C(47)	2 628(12)	7 193(8)	5 951(6)

two terminal carbonyl ligands. The remaining three carbonyl ligands are in bridging sites around three edges of the equatorial plane of the octahedral cluster core, with Ru– $\mu$ -C(O) distances lying in the range 1.94–2.41  $\text{\AA}$ . The fourth edge of the equatorial plane is occupied by a bridging AuP( $\text{C}_6\text{H}_4\text{Me}-2$ )<sub>3</sub> unit; Ru(3)–Au 2.782(1) and Ru(6)–Au 2.810(1)  $\text{\AA}$ . The Au–P vector lies nearly in the plane of atoms Ru(3), Ru(4), Ru(5) and Ru(6) with the P atom tipped slightly toward Ru(1) by 0.16  $\text{\AA}$ . The gold-bridged ruthenium–ruthenium edge is long [Ru(3)–Ru(6) 3.241(1)  $\text{\AA}$ ] but should be considered to be a bonding interaction if the Ru<sub>6</sub>-cluster core is to be consistent with an 86-valence-electron octahedral cage.

**Reaction of**  $[\text{Ru}_6\text{H}_2(\text{CO})_{18}\text{B}]^-$  **with**  $[\text{AuCl}(\text{PR}_3)]$  ( $\text{R} = \text{Ph}$  or 2-MeC<sub>6</sub>H<sub>4</sub>).—Treatment of anion **2** with an excess of  $[\text{AuCl}(\text{PPh}_3)]$  yields three related products:  $[\text{Ru}_6(\text{CO})_{17}\text{B}\{\text{Au}(\text{PPh}_3)\}]$  **4**,  $[\text{Ru}_6\text{H}(\text{CO})_{16}\text{B}\{\text{Au}(\text{PPh}_3)\}_2]$  **5** and  $[\text{Ru}_6(\text{CO})_{16}\text{B}\{\text{Au}(\text{PPh}_3)\}_3]$  **6**. In a stoichiometric reaction of **2** and  $[\text{AuCl}(\text{PPh}_3)]$ , the same three clusters are obtained but in lower yields. Each of clusters **4–6** has 86 electrons and possesses an octahedral cage in contrast to the trigonal-prismatic core of the starting material. Thus, **2** does not undergo the simple addition of a  $\text{Au}(\text{PPh}_3)^+$  electrophile to yield a neutral 90-electron cluster product. Instead, the reaction proceeds with loss of H<sub>2</sub> and CO accompanying the addition of one, two or three Au–PPh<sub>3</sub> fragments. The reaction of  $[\text{N}(\text{PPh}_3)_2]\text{[Ru}_6\text{H}_2(\text{CO})_{18}\text{B}]^-$  with  $[\text{AuCl}\{\text{P}(\text{C}_6\text{H}_4\text{Me}-2)\}_3]$  follows a similar pathway to that above but yields only the mono- and di-gold(I) phosphine products  $[\text{Ru}_6(\text{CO})_{17}\text{B}\{\text{AuP}(\text{C}_6\text{H}_4\text{Me}-2)\}_3]$  **7** and  $[\text{Ru}_6\text{H}(\text{CO})_{16}\text{B}\{\text{AuP}(\text{C}_6\text{H}_4\text{Me}-2)\}_2]$  **8**. Each of clusters **5**, **6** and **8** exhibits a resonance of similar shift in the <sup>11</sup>B NMR spectrum ( $\delta$  193.4, +194.2 and +194.0), and again these values reflect the presence of an Ru<sub>6</sub>B framework.

**Reactions of**  $[\text{Ru}_6(\text{CO})_{17}\text{B}]^-$  **and**  $[\text{Ru}_6\text{H}_2(\text{CO})_{18}\text{B}]^-$  **with**

**Table 5** Selected bond distances ( $\text{\AA}$ ) and angles ( $^\circ$ ) for compound 7

Au–Ru(3)	2.782(1)	Ru(2)–B	2.078(9)	Au–Ru(6)	2.810(1)	Ru(2)–Ru(6)	2.901(1)
Au–P	2.330(3)	Ru(3)–Ru(4)	2.840(1)	Ru(1)–Ru(3)	2.998(1)	Ru(3)–B	2.069(8)
Ru(1)–Ru(4)	2.979(1)	Ru(4)–Ru(5)	2.853(1)	Ru(1)–Ru(5)	2.872(1)	Ru(3)–Ru(6)	3.241(1)
Ru(1)–Ru(6)	2.949(1)	Ru(5)–Ru(6)	2.910(1)	Ru(1)–B	2.065(9)	Ru(4)–B	2.144(10)
Ru(2)–Ru(3)	2.917(1)	Ru(6)–B	2.067(10)	Ru(2)–Ru(4)	2.976(1)	Ru(5)–B	2.120(8)
Ru(2)–Ru(5)	2.993(1)						
Ru(3)–Au–Ru(6)	70.8(1)	Ru(4)–Ru(2)–Ru(6)	91.2(1)	Au–Ru(6)–Ru(5)	139.3(1)	Ru(3)–Ru(4)–B	46.5(2)
Ru(6)–Au–P	145.7(1)	Ru(3)–Ru(2)–B	45.2(2)	Ru(2)–Ru(6)–Ru(5)	62.0(1)	Ru(1)–Ru(5)–Ru(2)	89.8(1)
Ru(3)–Ru(1)–Ru(5)	90.5(1)	Ru(5)–Ru(2)–B	45.1(2)	Ru(1)–Ru(6)–B	44.4(3)	Ru(2)–Ru(5)–Ru(4)	61.1(1)
Ru(3)–Ru(1)–Ru(6)	66.0(1)	Au–Ru(3)–Ru(1)	93.2(1)	Ru(5)–Ru(6)–B	46.7(2)	Ru(2)–Ru(5)–Ru(6)	58.8(1)
Ru(5)–Ru(1)–Ru(6)	60.0(1)	Au–Ru(3)–Ru(2)	91.9(1)	Ru(1)–B–Ru(3)	92.9(4)	Ru(1)–Ru(5)–B	45.9(2)
Ru(4)–Ru(1)–B	46.0(3)	Au–Ru(3)–Ru(4)	142.1(1)	Ru(1)–B–Ru(4)	90.1(4)	Ru(4)–Ru(5)–B	48.3(3)
Ru(6)–Ru(1)–B	44.5(3)	Ru(2)–Ru(3)–Ru(4)	62.2(1)	Ru(2)–B–Ru(5)	91.0(4)	Au–Ru(6)–Ru(1)	93.7(1)
Ru(3)–Ru(2)–Ru(5)	89.7(1)	Ru(1)–Ru(3)–B	43.5(3)	Ru(3)–B–Ru(4)	84.7(3)	Ru(1)–Ru(6)–Ru(2)	90.1(1)
Ru(3)–Ru(2)–Ru(6)	67.7(1)	Ru(4)–Ru(3)–B	48.7(3)	Ru(4)–B–Ru(5)	84.0(4)	Ru(1)–Ru(6)–Ru(5)	58.7(1)
Ru(5)–Ru(2)–Ru(6)	59.2(1)	Ru(1)–Ru(4)–Ru(3)	62.0(1)	Ru(2)–B–Ru(6)	88.8(4)	Au–Ru(6)–B	92.6(2)
Ru(4)–Ru(2)–B	46.1(3)	Ru(1)–Ru(4)–Ru(5)	58.9(1)	Ru(4)–B–Ru(6)	171.9(5)	Ru(2)–Ru(6)–B	45.7(3)
Ru(6)–Ru(2)–B	45.4(3)	Ru(3)–Ru(4)–Ru(5)	94.2(1)	Ru(1)–Ru(3)–Ru(2)	88.9(1)	Ru(1)–B–Ru(2)	177.6(5)
Ru(3)–Au–P	143.3(1)	Ru(2)–Ru(4)–B	44.3(2)	Ru(1)–Ru(3)–Ru(4)	61.3(1)	Ru(2)–B–Ru(3)	89.4(3)
Ru(3)–Ru(1)–Ru(4)	56.7(1)	Ru(5)–Ru(4)–B	47.6(2)	Au–Ru(3)–B	93.4(3)	Ru(2)–B–Ru(4)	89.7(4)
Ru(4)–Ru(1)–Ru(5)	58.3(1)	Ru(1)–Ru(5)–Ru(4)	62.7(1)	Ru(2)–Ru(3)–B	45.4(3)	Ru(3)–B–Ru(5)	168.8(6)
Ru(4)–Ru(1)–Ru(6)	90.2(1)	Ru(1)–Ru(5)–Ru(6)	61.3(1)	Ru(1)–Ru(4)–Ru(2)	88.1(1)	Ru(1)–B–Ru(5)	86.7(3)
Ru(3)–Ru(1)–B	43.6(2)	Ru(4)–Ru(5)–Ru(6)	93.5(1)	Ru(2)–Ru(4)–Ru(3)	60.1(1)	Ru(1)–B–Ru(6)	91.1(4)
Ru(5)–Ru(1)–B	47.5(2)	Ru(2)–Ru(5)–B	44.0(2)	Ru(2)–Ru(4)–Ru(5)	61.7(1)	Ru(3)–B–Ru(6)	103.2(4)
Ru(3)–Ru(2)–Ru(4)	57.6(1)	Ru(6)–Ru(5)–B	45.2(3)	Ru(1)–Ru(4)–B	43.9(2)	Ru(5)–B–Ru(6)	88.1(3)
Ru(4)–Ru(2)–Ru(5)	57.1(1)	Au–Ru(6)–Ru(2)	91.6(1)				

**Table 6** Atomic coordinates ( $\times 10^4$ ) for compound 5

Atom	<i>x</i>	<i>y</i>	<i>z</i>	Atom	<i>x</i>	<i>y</i>	<i>z</i>
Au(1)	3 592(1)	6 539(1)	2 861(1)	C(502)	3 006(23)	7 001(17)	1 584(12)
Au(2)	5 909(1)	6 405(1)	2 101(1)	C(601)	1 729(36)	10 835(28)	1 537(20)
Ru(1)	5 567(2)	8 746(1)	1 764(1)	C(602)	3 667(28)	10 675(22)	773(14)
Ru(2)	2 186(2)	9 000(2)	2 816(1)	C(21)	3 619(14)	4 648(9)	4 413(8)
Ru(3)	3 765(2)	10 149(1)	2 824(1)	C(22)	4 028	3 938	4 909
Ru(4)	4 528(2)	7 976(1)	3 110(1)	C(23)	4 264	2 866	4 848
Ru(5)	3 953(2)	7 713(1)	1 633(1)	C(24)	4 091	2 503	4 290
Ru(6)	3 176(2)	9 931(2)	1 560(1)	C(25)	3 681	3 213	3 794
P(1)	2 857(5)	5 222(5)	3 235(3)	C(26)	3 445	4 285	3 856
P(2)	7 534(5)	4 885(5)	1 988(3)	C(31)	2 143(12)	3 971(13)	2 580(8)
B	3 887(21)	8 819(19)	2 288(12)	C(32)	2 283	3 330	2 053
O(1)	2 868(21)	8 742(16)	495(10)	C(33)	3 247	3 145	1 489
O(2)	4 719(19)	9 363(14)	4 056(9)	C(34)	4 071	3 601	1 452
C(1)	3 137(24)	8 815(20)	984(14)	C(35)	3 931	4 242	1 979
C(2)	4 482(22)	9 235(17)	3 594(12)	C(36)	2 967	4 427	2 544
O(101)	5 939(20)	10 636(17)	956(12)	C(41)	823(14)	5 819(14)	4 310(8)
O(102)	7 400(19)	7 327(18)	579(11)	C(42)	-367	6 385	4 578
O(103)	7 434(15)	8 597(14)	2 442(9)	C(43)	-1 061	6 966	4 148
O(201)	405(22)	11 177(21)	3 213(18)	C(44)	-564	6 982	3 449
O(202)	473(18)	8 644(16)	2 209(12)	C(45)	626	6 416	3 180
O(203)	1 184(18)	8 138(18)	4 158(11)	C(46)	1 320	5 835	3 611
O(301)	5 349(17)	11 405(15)	2 557(10)	C(51)	9 042(13)	5 926(11)	1 701(8)
O(302)	1 975(19)	11 848(17)	3 809(11)	C(52)	10 072	6 101	1 373
O(401)	3 534(15)	7 233(15)	4 485(9)	C(53)	10 929	5 397	878
O(402)	6 880(15)	6 800(15)	3 386(8)	C(54)	10 757	4 518	712
O(501)	5 600(21)	6 523(18)	380(10)	C(55)	9 728	4 343	1 039
O(502)	2 434(18)	6 547(16)	1 486(10)	C(56)	8 870	5 047	1 534
O(601)	780(24)	11 384(21)	1 545(15)	C(61)	6 883(11)	4 165(14)	3 294(8)
O(602)	3 940(22)	11 074(16)	306(11)	C(62)	7 056	3 749	3 925
C(101)	5 732(23)	9 921(21)	1 258(13)	C(63)	8 142	3 504	4 057
C(102)	6 686(25)	7 835(21)	1 017(15)	C(64)	9 055	3 674	3 557
C(103)	6 718(19)	8 619(18)	2 194(11)	C(65)	8 882	4 089	2 926
C(201)	1 113(26)	10 344(30)	3 056(19)	C(66)	7 796	4 335	2 795
C(202)	1 169(24)	8 737(21)	2 398(14)	C(71)	7 685(17)	2 829(14)	1 826(8)
C(203)	1 625(23)	8 400(22)	3 630(16)	C(72)	7 623	2 045	1 474
C(301)	4 771(21)	10 938(18)	2 658(11)	C(73)	7 339	2 277	850
C(302)	2 572(24)	11 226(22)	3 443(13)	C(74)	7 117	3 293	579
C(401)	3 871(20)	7 487(19)	3 961(11)	C(75)	7 178	4 078	932
C(402)	6 006(19)	7 245(18)	3 260(11)	C(76)	7 462	3 846	1 555
C(501)	4 977(24)	6 964(21)	877(13)				

$\{[(R_3P)Au]_3O\}[BF_4]$  ( $R = \text{Ph or } 2\text{-MeC}_6\text{H}_4$ ).—Trigold oxonium salts are useful synthetic reagents for the introduction into a cluster of up to three gold(I) phosphine units.<sup>34</sup> Despite the fact that  $[\text{Ru}_6(\text{CO})_{16}\text{B}\{\text{Au}(\text{PPh}_3)\}_3]$  **6** can be prepared from the reaction of anion **2** with an excess of  $[\text{AuCl}(\text{PPh}_3)]$ , we were unable to prepare  $[\text{Ru}_6(\text{CO})_{16}\text{B}\{\text{AuP}(\text{C}_6\text{H}_4\text{Me}-2)_3\}_3]$  by an analogous route. The use of  $\{[(2\text{-MeC}_6\text{H}_4)_3\text{PAu}]_3O\}[BF_4]$  was therefore investigated. First, we showed that  $\{[(\text{Ph}_3\text{P})\text{Au}]_3O\}[BF_4]$  can be successfully used to synthesise the trigold derivative **6**. The reaction of the octahedral anion **1** with  $\{[(\text{Ph}_3\text{P})\text{Au}]_3O\}[BF_4]$  produces both **4** and **6** in relatively good yields. However, the trigonal-prismatic boride anion **2** reacts with  $\{[(\text{Ph}_3\text{P})\text{Au}]_3O\}[BF_4]$  to give **6** in poor yield. When **1** reacts with  $\{[(2\text{-MeC}_6\text{H}_4)_3\text{PAu}]_3O\}[BF_4]$  the monogold derivative **7** and the trigold cluster  $[\text{Ru}_6(\text{CO})_{16}\text{B}\{\text{AuP}(\text{C}_6\text{H}_4\text{Me}-2)_3\}_3]$  **9** are formed. In the present study, this route gives the only method of preparing **9**. Attempts to form **9** by treating anion **2** with  $\{[(2\text{-MeC}_6\text{H}_4)_3\text{PAu}]_3O\}[BF_4]$  leads only to numerous, unidentified products in very low yields, in addition to  $[\text{Ru}_4\text{H}_3(\text{CO})_{12}\{\text{AuP}(\text{C}_6\text{H}_4\text{Me}-2)_3\}]$  (see Experimental section).

**Molecular Structure of  $[\text{Ru}_6\text{H}(\text{CO})_{16}\text{B}\{\text{Au}(\text{PPh}_3)\}_2]$  **5**.**—A crystal of compound **5** suitable for X-ray diffraction analysis was grown from  $\text{CH}_2\text{Cl}_2$  layered with hexane. The molecular structure is illustrated in Fig. 3; atomic coordinates are given in Table 6 and selected bond distances and angles in Table 7. The central  $\text{Ru}_6$  cage is distorted octahedral; one edge,  $\text{Ru}(4)-\text{Ru}(5)$ , is of length  $3.389(2)$  Å compared with a range of  $\text{Ru}-\text{Ru}$  distances of  $2.810(3)$ – $2.992(3)$  Å for the remaining eleven edges. As in **7**, **5** has an 86-electron count consistent with an octahedral cluster, but the edge  $\text{Ru}(4)-\text{Ru}(5)$ , which is associated with the gold(I) phosphine fragments, is lengthened. The boron atom resides in an interstitial position and interacts similarly with all six ruthenium atoms [ $\text{Ru}-\text{B } 2.06(2)$ – $2.15(3)$  Å]. Each of atoms  $\text{Ru}(1)$  and  $\text{Ru}(2)$  bears three terminal carbonyl ligands while

$\text{Ru}(3), \text{Ru}(4), \text{Ru}(5)$  and  $\text{Ru}(6)$  each carries two. The remaining two carbonyl ligands bridge edges  $\text{Ru}(3)-\text{Ru}(4)$  and  $\text{Ru}(5)-\text{Ru}(6)$  with distances  $\text{Ru}(3)-\text{C}(2) 2.10(2)$ ,  $\text{Ru}(4)-\text{C}(2) 2.06(3)$ ,  $\text{Ru}(5)-\text{C}(1) 2.06(3)$  and  $\text{Ru}(6)-\text{C}(1) 2.05(3)$  Å.

Each  $\text{Au}(\text{PPh}_3)$  fragment caps an  $\text{Ru}_3$  face of the central octahedron; the two capped faces are adjacent and the  $\text{Au}-\text{Au}$  separation of  $2.878(1)$  Å indicates a bonding interaction. This is at the expense of two more efficient  $\text{Au}-\text{Ru}$  interactions since the gold atoms are displaced towards one another and away from atoms  $\text{Ru}(1)$  and  $\text{Ru}(2)$  respectively [Fig. 4(b)];  $\text{Au}(1)-\text{Ru}(2) 3.169(2)$  and  $\text{Au}(2)-\text{Ru}(1) 3.094(2)$  Å]. The lengthening of edge  $\text{Ru}(4)-\text{Ru}(5)$  appears to be a further consequence of the  $\text{Au}-\text{Au}$  interaction. Molecule **5** possesses an approximate two-fold axis which runs through the midpoint

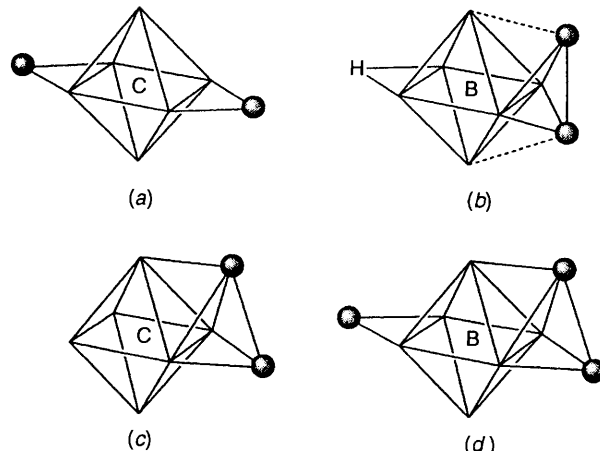


Fig. 4 Core structures of (a)  $[\text{Ru}_6(\text{CO})_{16}\text{C}\{\text{Au}(\text{PMePh}_2)\}_2]$ ,<sup>35</sup> (b)  $[\text{Ru}_6\text{H}(\text{CO})_{16}\text{B}\{\text{Au}(\text{PPh}_3)\}_2]$  **5**, (c)  $[\text{Ru}_6(\text{CO})_{16}\text{C}\{\text{Cu}(\text{NCMe})\}_2]$ ,<sup>36</sup> and (d)  $[\text{Ru}_6(\text{CO})_{16}\text{B}\{\text{Au}(\text{PPh}_3)\}_3]$  **6**

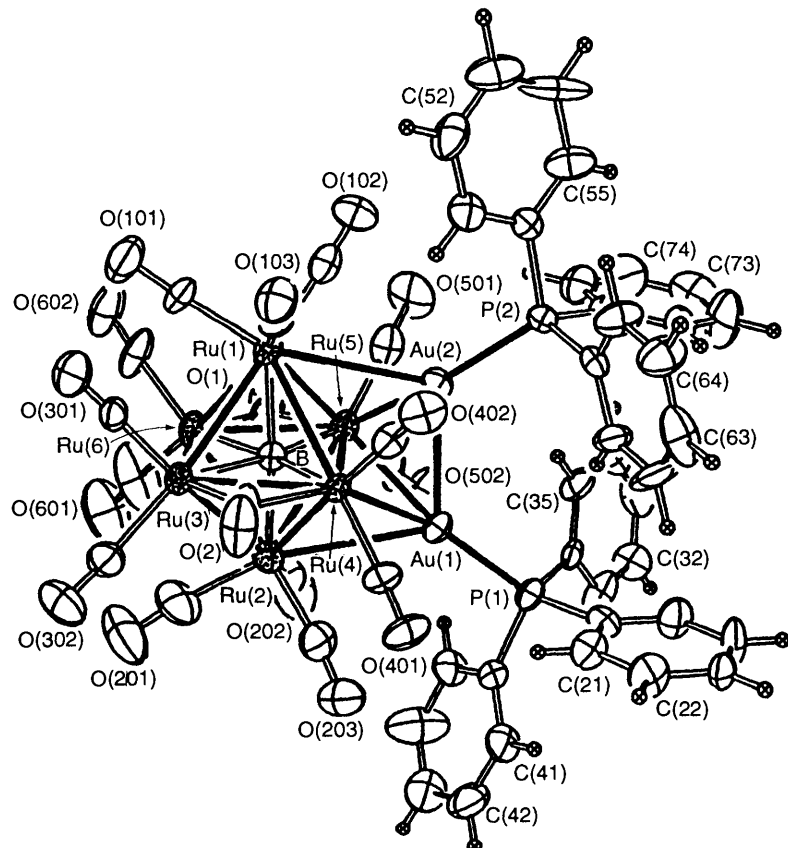
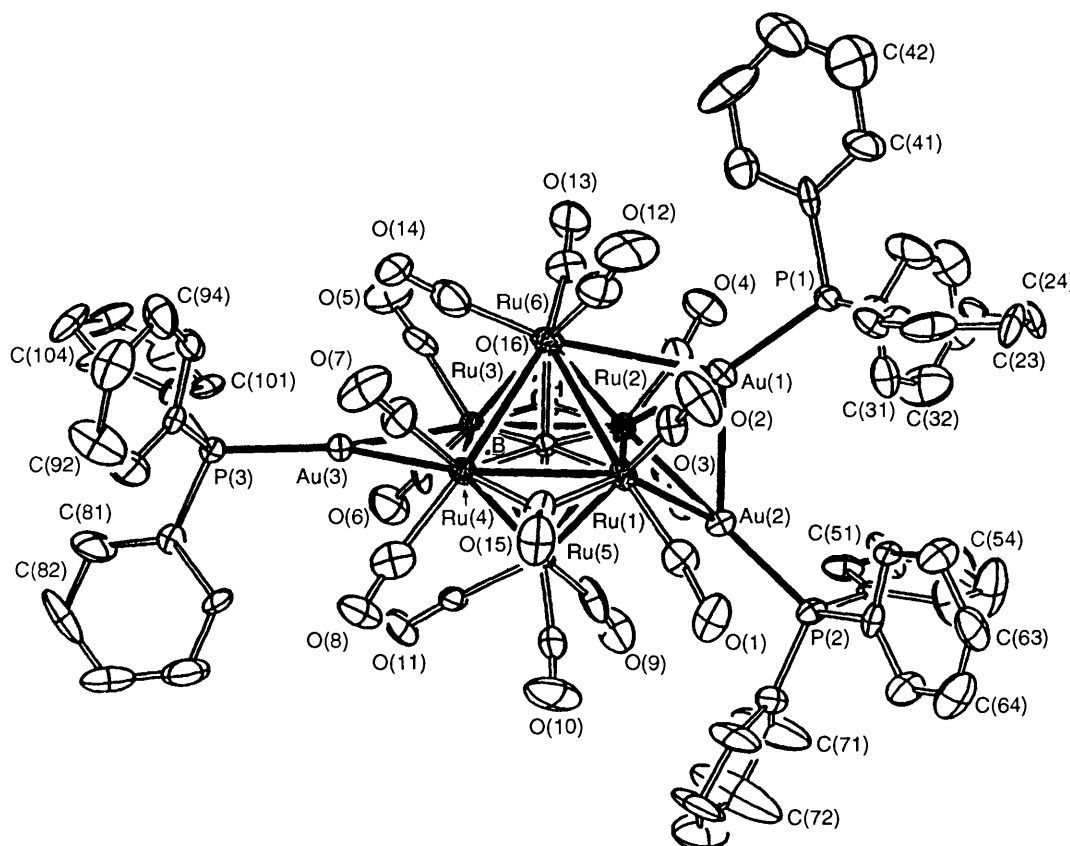


Fig. 3 Molecular structure of  $[\text{Ru}_6\text{H}(\text{CO})_{16}\text{B}\{\text{Au}(\text{PPh}_3)\}_2]$  **5**

Fig. 5 Molecular structure of  $[\text{Ru}_6(\text{CO})_{16}\text{B}\{\text{Au}(\text{PPh}_3)\}_3]$  6Table 7 Selected bond distances ( $\text{\AA}$ ) and angles ( $^\circ$ ) for compound 5

Au(1)-Au(2)	2.878(1)	Ru(1)-B	2.09(3)	Au(1)-Ru(4)	2.811(3)	Ru(2)-Ru(4)	2.987(3)
Au(1)-Ru(5)	2.855(2)	Ru(2)-Ru(5)	2.988(2)	Au(1)-P(1)	2.301(7)	Ru(2)-Ru(6)	2.919(3)
Au(1)-Ru(2)	3.169(2)	Ru(2)-B	2.06(3)	Au(2)-Ru(4)	2.838(2)	Ru(3)-Ru(4)	2.810(3)
Au(2)-Ru(5)	2.819(2)	Ru(3)-Ru(6)	2.962(3)	Au(2)-Ru(1)	3.094(2)	Ru(3)-B	2.15(3)
Au(2)-P(2)	2.293(5)	Ru(4)-B	2.11(3)	Ru(1)-Ru(3)	2.910(2)	Ru(5)-Ru(6)	2.817(3)
Ru(1)-Ru(4)	2.975(2)	Ru(5)-B	2.11(3)	Ru(1)-Ru(5)	2.988(3)	Ru(6)-B	2.15(3)
Ru(1)-Ru(6)	2.992(3)	Ru(4)-Ru(5)	3.389(2)	Ru(2)-Ru(3)	2.992(4)		
Au(2)-Au(1)-Ru(2)	101.1(1)	Ru(4)-Ru(2)-Ru(5)	69.1(1)	Ru(4)-Ru(2)-Ru(6)	91.6(1)	Ru(5)-Ru(6)-B	48.0(8)
Ru(2)-Au(1)-Ru(4)	59.6(1)	Ru(3)-Ru(2)-Ru(6)	60.1(1)	Au(1)-Ru(2)-B	76.0(7)	Ru(1)-B-Ru(3)	86.7(12)
Ru(2)-Au(1)-Ru(5)	59.2(1)	Ru(5)-Ru(2)-Ru(6)	56.9(1)	Ru(4)-Ru(2)-B	44.8(7)	Ru(1)-B-Ru(4)	90.3(10)
Au(2)-Au(1)-P(1)	130.1(1)	Ru(3)-Ru(2)-B	45.8(8)	Ru(6)-Ru(2)-B	47.3(7)	Ru(3)-B-Ru(4)	82.7(11)
Ru(4)-Au(1)-P(1)	150.1(2)	Ru(5)-Ru(2)-B	44.8(8)	Ru(1)-Ru(3)-Ru(4)	62.7(1)	Ru(2)-B-Ru(5)	91.5(13)
Au(1)-Au(2)-Ru(1)	102.4(1)	Ru(1)-Ru(3)-Ru(2)	89.4(1)	Ru(1)-Ru(3)-Ru(6)	61.3(1)	Ru(4)-B-Ru(5)	107.1(11)
Ru(1)-Au(2)-Ru(4)	60.0(1)	Ru(2)-Ru(3)-Ru(4)	61.9(1)	Ru(4)-Ru(3)-Ru(6)	94.4(1)	Ru(2)-B-Ru(6)	87.8(10)
Ru(1)-Au(2)-Ru(5)	60.5(1)	Ru(2)-Ru(3)-Ru(6)	58.7(1)	Ru(2)-Ru(3)-B	43.6(7)	Ru(4)-B-Ru(6)	169.9(16)
Au(1)-Au(2)-P(2)	123.7(2)	Ru(1)-Ru(3)-B	45.8(7)	Ru(6)-Ru(3)-B	46.3(7)	Au(1)-Ru(5)-Au(2)	61.0(1)
Au(2)-Au(1)-Ru(4)	59.8(1)	Ru(4)-Ru(3)-B	48.0(7)	Au(1)-Ru(4)-Ru(1)	107.1(1)	Au(2)-Ru(5)-Ru(1)	64.3(1)
Au(2)-Au(1)-Ru(5)	58.9(1)	Au(1)-Ru(4)-Au(2)	61.2(1)	Au(1)-Ru(4)-Ru(2)	66.2(1)	Au(2)-Ru(5)-Ru(2)	107.1(1)
Ru(4)-Au(1)-Ru(5)	73.5(1)	Au(2)-Ru(4)-Ru(1)	64.3(1)	Ru(1)-Ru(4)-Ru(2)	88.3(1)	Au(1)-Ru(5)-Ru(6)	124.4(1)
Ru(2)-Au(1)-P(1)	128.0(1)	Au(2)-Ru(4)-Ru(2)	106.6(1)	Au(2)-Ru(4)-Ru(3)	123.4(1)	Ru(2)-Ru(5)-Ru(6)	60.3(1)
Ru(5)-Au(1)-P(1)	136.4(2)	Au(1)-Ru(4)-Ru(3)	126.7(1)	Ru(2)-Ru(4)-Ru(3)	62.1(1)	Au(2)-Ru(5)-B	83.6(7)
Au(1)-Au(2)-Ru(4)	58.9(1)	Ru(1)-Ru(4)-Ru(3)	60.3(1)	Au(2)-Ru(4)-B	83.1(6)	Ru(2)-Ru(5)-B	43.6(7)
Au(1)-Au(2)-Ru(5)	60.1(1)	Au(1)-Ru(4)-B	84.2(9)	Ru(2)-Ru(4)-B	43.7(7)	Ru(1)-Ru(6)-Ru(2)	89.2(1)
Ru(4)-Au(2)-Ru(5)	73.6(1)	Ru(1)-Ru(4)-B	44.6(7)	Ru(3)-Ru(4)-B	49.3(8)	Ru(2)-Ru(6)-Ru(3)	61.2(1)
Ru(1)-Au(2)-P(2)	133.2(2)	Ru(5)-Au(2)-P(2)	149.0(2)	Au(1)-Ru(5)-Ru(1)	105.6(1)	Ru(2)-Ru(6)-Ru(5)	62.8(1)
Ru(4)-Au(2)-P(2)	136.7(2)	Au(2)-Ru(1)-Ru(4)	55.7(1)	Au(1)-Ru(5)-Ru(2)	65.6(1)	Ru(1)-Ru(6)-B	44.3(7)
Au(2)-Ru(1)-Ru(3)	111.8(1)	Au(2)-Ru(1)-Ru(5)	55.2(1)	Ru(1)-Ru(5)-Ru(2)	88.0(1)	Ru(3)-Ru(6)-B	46.4(8)
Ru(3)-Ru(1)-Ru(4)	57.0(1)	Ru(4)-Ru(1)-Ru(5)	69.3(1)	Ru(1)-Ru(5)-Ru(6)	62.0(1)	Ru(1)-B-Ru(2)	176.1(15)
Ru(3)-Ru(1)-Ru(5)	91.9(1)	Ru(3)-Ru(1)-Ru(6)	60.2(1)	Au(1)-Ru(5)-B	83.0(7)	Ru(2)-B-Ru(3)	90.6(8)
Au(2)-Ru(1)-Ru(6)	110.3(1)	Ru(5)-Ru(1)-Ru(6)	56.2(1)	Ru(1)-Ru(5)-B	44.4(7)	Ru(2)-B-Ru(4)	91.5(9)
Ru(4)-Ru(1)-Ru(6)	90.4(1)	Ru(3)-Ru(1)-B	47.5(8)	Ru(6)-Ru(5)-B	49.1(7)	Ru(1)-B-Ru(5)	90.8(8)
Au(2)-Ru(1)-B	77.1(7)	Ru(5)-Ru(1)-B	44.9(8)	Ru(1)-Ru(6)-Ru(3)	58.5(1)	Ru(3)-B-Ru(5)	169.9(13)
Ru(4)-Ru(1)-B	45.1(7)	Au(1)-Ru(2)-Ru(3)	109.2(1)	Ru(1)-Ru(6)-Ru(5)	61.8(1)	Ru(1)-B-Ru(6)	89.9(10)
Ru(6)-Ru(1)-B	45.8(7)	Ru(3)-Ru(2)-Ru(4)	56.1(1)	Ru(3)-Ru(6)-Ru(5)	94.3(1)	Ru(3)-B-Ru(6)	87.3(9)
Au(1)-Ru(2)-Ru(4)	54.2(1)	Ru(3)-Ru(2)-Ru(5)	90.3(1)	Ru(2)-Ru(6)-B	44.9(7)	Ru(5)-B-Ru(6)	82.9(10)
Au(1)-Ru(2)-Ru(5)	55.2(1)	Au(1)-Ru(2)-Ru(6)	111.0(1)				

**Table 8** Atomic coordinates ( $\times 10^4$ ) for compound **6**

Atom	<i>x</i>	<i>y</i>	<i>z</i>	Atom	<i>x</i>	<i>y</i>	<i>z</i>
Au(1)	2558.6(6)	5001.06(6)	1741.3(5)	C(26)	2224	5523	262
Au(2)	3943.1(6)	531.07(6)	2271.3(5)	C(31)	3462(11)	4141(11)	672(9)
Au(3)	2201.5(6)	5125.1(6)	4776.8(5)	C(32)	3914	3666	446
Ru(1)	2811.3(12)	6030.5(12)	2659.5(9)	C(33)	3668	3115	47
Ru(2)	3182.9(12)	4284.3(11)	2796.1(9)	C(34)	2970	3038	-126
Ru(3)	2711.7(12)	4309.5(12)	3915.7(10)	C(35)	2519	3512	100
Ru(4)	2369.3(12)	5980.7(11)	3782.6(10)	C(36)	2765	4064	499
Ru(5)	3732.7(12)	5420.8(12)	3702.6(10)	C(41)	993(13)	4484(12)	10(8)
Ru(6)	1801.3(12)	4874.2(12)	2895.7(11)	C(42)	352	4169	-134
P(1)	2110(4)	4739(4)	752(3)	C(43)	76	3749	288
P(2)	4894(4)	5692(4)	1879(3)	C(44)	441	3644	854
P(3)	1793(4)	5308(4)	5663(3)	C(45)	1082	3959	998
B	2745(16)	5122(15)	3287(13)	C(46)	1358	4379	576
O(1)	3837(13)	7155(11)	2360(10)	C(51)	5325(11)	4296(10)	1682(8)
O(2)	1873(13)	6826(12)	1723(10)	C(52)	5626	3754	1373
O(3)	4525(12)	3562(12)	2762(9)	C(53)	5852	3920	831
O(4)	2663(13)	3179(12)	1879(10)	C(54)	5776	4629	600
O(5)	1538(13)	3367(12)	4192(12)	C(55)	5475	5171	909
O(6)	3584(15)	3793(13)	5029(11)	C(56)	5249	5005	1450
O(7)	1023(13)	6614(12)	3960(13)	C(61)	4056(8)	6452(9)	1024(8)
O(8)	3019(12)	6862(12)	4843(10)	C(62)	3881	7027	627
O(9)	5115(13)	4718(16)	3616(11)	C(63)	4347	7583	567
O(10)	4301(16)	6965(13)	3817(12)	C(64)	4989	7565	905
O(11)	4098(12)	5388(13)	5049(9)	C(65)	5165	6990	1303
O(12)	855(13)	5614(17)	1877(15)	C(66)	4699	6433	1363
O(13)	1340(13)	3320(12)	2537(10)	C(71)	6109(13)	5623(13)	2651(12)
O(14)	704(13)	4870(16)	3694(12)	C(72)	6573	5867	3130
O(15)	2476(12)	7451(11)	3206(9)	C(73)	6457	6524	3415
O(16)	3201(13)	2873(11)	3489(9)	C(74)	5877	6936	3221
C(1)	3441(18)	6677(15)	2448(13)	C(75)	5414	6691	2742
C(2)	2225(17)	6488(16)	2053(13)	C(76)	5530	6034	2457
C(3)	4019(16)	3855(15)	2768(11)	C(81)	2281(9)	5657(12)	6842(9)
C(4)	2914(19)	3640(16)	2216(14)	C(82)	2744	5974	7289
C(5)	1960(18)	3739(16)	4069(13)	C(83)	3343	6282	7147
C(6)	3231(20)	4016(18)	4580(13)	C(84)	3480	6273	6559
C(7)	1501(19)	6351(18)	3909(15)	C(85)	3017	5956	6112
C(8)	2787(16)	6521(17)	4494(17)	C(86)	2417	5648	6253
C(9)	4584(22)	4949(18)	3607(13)	C(91)	1159(9)	6642(10)	5878(9)
C(10)	4110(19)	6386(21)	3752(13)	C(92)	622	7140	5800
C(11)	3947(15)	5373(16)	4545(13)	C(93)	28	6968	5421
C(12)	1235(21)	5374(19)	2247(17)	C(94)	-28	6299	5120
C(13)	1538(17)	3895(17)	2650(15)	C(95)	509	5801	5199
C(14)	1118(21)	4895(19)	3408(16)	C(96)	1103	5973	5578
C(15)	2523(15)	6820(14)	3212(12)	C(101)	1766(9)	3837(12)	5865(9)
C(16)	3080(16)	3482(15)	3448(11)	C(102)	1560	3201	6131
C(21)	1907(10)	6170(11)	399(7)	C(103)	1032	3229	6476
C(22)	1824	6742	-14	C(104)	709	3893	6555
C(23)	2059	6666	-564	C(105)	915	4529	6289
C(24)	2377	6018	-700	C(106)	1444	4501	5944
C(25)	2459	5446	-287				

of Au(1)–Au(2), the boron atom, and the midpoint of Ru(3)–Ru(6). The  $^1\text{H}$  NMR spectrum indicates the presence of a hydride ligand but this was not located directly. However, consideration of the cluster-electron count, cluster symmetry, and the orientation of the carbonyl ligands suggests the placement of a single hydride ligand bridging edge Ru(3)–Ru(6). This is consistent with the observed  $^1\text{H}$  NMR spectral shift of  $\delta = -14.47$ .

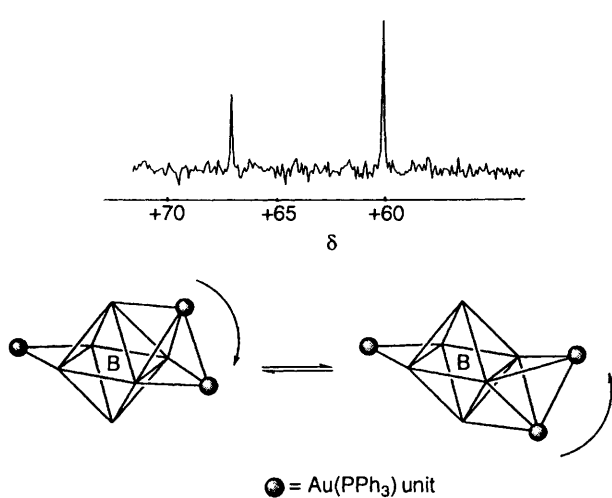
Cluster **5** is isoelectronic with  $[\text{Ru}_6(\text{CO})_{16}\text{C}\{\text{Au}(\text{PMePh}_2)\}_2]$ ,<sup>35</sup> with the interstitial carbon atom in the latter being replaced in **5** by the boron atom plus the external hydride ligand. The solid-state structures of  $[\text{Ru}_6(\text{CO})_{16}\text{C}\{\text{Au}(\text{PMePh}_2)\}_2]$  and **5** show significant differences [Fig. 4(a) and 4(b)]; in contrast to **5**, the two gold(i) phosphine units in  $[\text{Ru}_6(\text{CO})_{16}\text{C}\{\text{Au}(\text{PMePh}_2)\}_2]$  are remote from one another. The role of the additional hydride ligand may be influential in causing this structural difference and indeed we have commented on this factor previously in a comparison of the structures of  $[\text{Fe}_4(\text{CO})_{12}\text{BH}\{\text{Au}(\text{PR}_3)\}_2]$  (*e.g.* R = Ph or Et) and  $[\text{Fe}_4(\text{CO})_{12}\text{C}\{\text{Au}(\text{PEt}_3)\}_2]$ .<sup>37,38</sup> On the other hand, the

relative positions of the two copper(i) fragments in the analogous cluster  $[\text{Ru}_6(\text{CO})_{16}\text{C}\{\text{Cu}(\text{NCMe})\}_2]$ <sup>36</sup> [Fig. 4(c)] quite closely resemble those of the gold(i) units in **5** although here the dicopper unit favours an asymmetrical orientation with respect to the  $\text{Ru}_6\text{C}$  core with  $\text{Ru}_{\text{apex}}\text{–Cu}$  distances of 2.741(1) and 3.376(1) Å. A similar asymmetrical arrangement is observed for the digold unit in  $[\text{Ru}_5\text{W}(\text{CO})_{17}\text{C}\{\text{Au}(\text{PEt}_3)\}_2]$ ,<sup>35</sup> and solution  $^{31}\text{P}$  NMR spectroscopic data suggest the presence of second isomer of  $[\text{Ru}_6(\text{CO})_{16}\text{C}\{\text{Au}(\text{PMePh}_2)\}_2]$  which adopts this arrangement of heavy-metal fragments.<sup>35</sup> We would agree with a previous conclusion by Bradley *et al.*<sup>36</sup> that the reasons for structural preferences in this series of clusters are not clear.

*Molecular Structure of  $[\text{Ru}_6(\text{CO})_{16}\text{B}\{\text{Au}(\text{PPh}_3)\}_3]$ .*—A crystal of compound **6** suitable for X-ray diffraction analysis was grown from  $\text{CH}_2\text{Cl}_2$  layered with hexane. The molecular structure is shown in Fig. 5; atomic coordinates are listed in Table 8 and selected bond distances and angles in Table 9. The  $\text{Ru}_6$  core of **6** comprises an octahedron in keeping with the 86-electron cluster count, although, as in **5** and **7**, association of

**Table 9** Selected bond distances ( $\text{\AA}$ ) and angles ( $^\circ$ ) for compound **6**

Au(1)–Au(2)	2.899(2)	Ru(1)–B	2.20(3)	Au(1)–Ru(1)	2.782(2)	Ru(2)–Ru(3)	2.821(3)
Au(1)–Ru(2)	2.858(2)	Ru(2)–Ru(5)	3.014(3)	Au(1)–Ru(6)	3.201(3)	Ru(2)–Ru(6)	2.990(3)
Au(1)–P(1)	2.303(7)	Ru(2)–B	2.15(3)	Au(2)–Ru(1)	2.849(3)	Ru(3)–Ru(4)	3.130(3)
Au(2)–Ru(2)	2.776(3)	Ru(3)–Ru(5)	2.957(3)	Au(2)–P(2)	2.306(8)	Ru(3)–Ru(6)	2.916(3)
Au(3)–Ru(3)	2.755(3)	Ru(3)–B	2.06(3)	Au(3)–Ru(4)	2.796(3)	Ru(4)–Ru(5)	2.928(3)
Au(3)–P(3)	2.291(8)	Ru(4)–B	2.958(3)	Ru(1)–Ru(4)	2.803(3)	Ru(4)–B	2.12(3)
Ru(1)–Ru(5)	2.994(3)	Ru(5)–B	2.13(3)	Ru(1)–Ru(6)	3.013(3)	Ru(6)–B	2.01(3)
Au(2)–Au(1)–Ru(1)	60.2(1)	Au(1)–Ru(2)–B	86.6(7)	Au(2)–Ru(2)–B	91.4(8)	Ru(1)–Ru(6)–B	46.9(8)
Ru(1)–Au(1)–Ru(2)	71.0(1)	Ru(3)–Ru(2)–B	46.6(8)	Ru(5)–Ru(2)–B	44.9(8)	Ru(3)–Ru(6)–B	45.0(8)
Ru(1)–Au(1)–Ru(6)	60.0(1)	Ru(6)–Ru(2)–B	42.3(8)	Au(3)–Ru(3)–Ru(2)	147.7(1)	Ru(1)–B–Ru(2)	97.9(12)
Au(2)–Au(1)–P(1)	125.6(2)	Au(3)–Ru(3)–Ru(4)	56.3(1)	Au(3)–Ru(3)–Ru(6)	96.8(1)	Ru(1)–B–Ru(3)	176.6(16)
Au(1)–Au(2)–Ru(2)	60.4(2)	Ru(2)–Ru(3)–Ru(4)	91.4(1)	Au(3)–Ru(3)–Ru(5)	94.2(1)	Ru(1)–B–Ru(4)	80.9(9)
Au(2)–Au(2)–P(2)	132.9(2)	Ru(2)–Ru(3)–Ru(5)	62.8(1)	Ru(4)–Ru(3)–Ru(5)	57.4(1)	Ru(3)–B–Ru(4)	96.9(12)
Ru(3)–Au(3)–P(3)	155.2(2)	Ru(2)–Ru(3)–Ru(6)	62.8(1)	Ru(5)–Ru(3)–Ru(6)	89.6(1)	Ru(2)–B–Ru(5)	89.7(12)
Au(1)–Ru(1)–Ru(4)	127.5(1)	Ru(4)–Ru(3)–Ru(6)	58.4(1)	Au(3)–Ru(3)–B	98.6(8)	Ru(4)–B–Ru(5)	87.1(10)
Au(1)–Ru(1)–Ru(5)	111.5(1)	Ru(2)–Ru(3)–B	49.1(8)	Ru(4)–Ru(3)–B	42.3(8)	Ru(2)–B–Ru(6)	91.9(11)
Ru(4)–Ru(1)–Ru(5)	60.6(1)	Ru(5)–Ru(3)–B	46.0(8)	Ru(6)–Ru(3)–B	43.6(8)	Ru(4)–B–Ru(6)	91.3(13)
Au(2)–Au(1)–Ru(2)	57.6(1)	Au(3)–Ru(4)–Ru(1)	146.6(1)	Au(3)–Ru(4)–Ru(6)	95.0(1)	Ru(2)–Ru(5)–Ru(4)	91.8(1)
Au(2)–Au(1)–Ru(6)	101.8(1)	Au(3)–Ru(4)–Ru(3)	55.1(1)	Ru(1)–Ru(4)–Ru(3)	91.6(1)	Ru(1)–Ru(5)–B	47.2(8)
Ru(2)–Au(1)–Ru(6)	58.8(1)	Au(3)–Ru(4)–Ru(5)	94.0(1)	Ru(1)–Ru(4)–Ru(5)	62.9(1)	Ru(3)–Ru(5)–B	44.2(8)
Au(1)–Au(2)–Ru(1)	57.9(1)	Ru(3)–Ru(4)–Ru(5)	58.3(1)	Ru(1)–Ru(4)–Ru(6)	63.0(1)	Au(1)–Ru(6)–B	79.9(9)
Ru(1)–Au(2)–Ru(2)	71.2(1)	Ru(3)–Ru(4)–Ru(6)	57.2(1)	Ru(5)–Ru(4)–Ru(6)	89.4(1)	Au(1)–Ru(6)–Ru(2)	54.9(1)
Ru(3)–Au(3)–Ru(4)	68.7(1)	Au(3)–Ru(4)–B	95.9(8)	Ru(1)–Ru(4)–B	50.8(8)	Au(1)–Ru(6)–Ru(3)	111.2(1)
Ru(4)–Au(3)–P(3)	136.0(2)	Ru(3)–Ru(4)–B	40.8(8)	Ru(5)–Ru(4)–B	46.5(8)	Ru(2)–Ru(6)–Ru(3)	57.1(1)
Au(2)–Ru(1)–Ru(4)	128.7(1)	Ru(6)–Ru(4)–B	42.9(8)	Ru(1)–Ru(5)–Ru(3)	91.4(1)	Ru(1)–Ru(6)–Ru(4)	56.0(1)
Au(2)–Ru(1)–Ru(5)	69.4(1)	Ru(1)–Ru(5)–Ru(2)	66.1(1)	Ru(2)–Ru(5)–Ru(3)	56.4(1)	Ru(3)–Ru(6)–Ru(4)	64.4(1)
Au(1)–Ru(1)–Ru(6)	66.9(1)	Ru(4)–Ru(1)–Ru(6)	61.0(1)	Ru(1)–Ru(5)–Ru(4)	56.5(1)	Ru(2)–Ru(6)–B	45.8(8)
Au(2)–Ru(1)–Ru(6)	107.9(1)	Au(1)–Ru(1)–B	87.5(7)	Ru(3)–Ru(5)–Ru(4)	64.3(1)	Ru(4)–Ru(6)–B	45.8(8)
Ru(5)–Ru(1)–Ru(6)	87.1(1)	Ru(4)–Ru(1)–B	48.4(8)	Ru(2)–Ru(5)–B	45.4(8)	Ru(5)–B–Ru(6)	178.1(16)
Au(2)–Ru(1)–B	88.4(8)	Ru(6)–Ru(1)–B	41.9(8)	Ru(4)–Ru(5)–B	46.4(8)	Ru(2)–B–Ru(3)	84.2(10)
Ru(5)–Ru(1)–B	45.2(8)	Au(1)–Ru(2)–Ru(3)	125.6(1)	Au(1)–Ru(6)–Ru(1)	53.1(1)	Ru(2)–B–Ru(4)	176.6(17)
Au(1)–Ru(2)–Au(2)	61.9(1)	Au(1)–Ru(2)–Ru(5)	108.9(1)	Ru(1)–Ru(6)–Ru(2)	66.2(1)	Ru(1)–B–Ru(5)	87.6(11)
Au(2)–Ru(2)–Ru(3)	129.9(1)	Ru(3)–Ru(2)–Ru(5)	60.8(1)	Ru(1)–Ru(6)–Ru(3)	91.8(1)	Ru(3)–B–Ru(5)	89.8(11)
Au(2)–Ru(2)–Ru(5)	70.1(1)	Au(2)–Ru(2)–Ru(6)	110.5(1)	Au(1)–Ru(6)–Ru(4)	108.8(1)	Ru(1)–B–Ru(6)	91.2(11)
Au(1)–Ru(2)–Ru(6)	66.3(1)	Ru(5)–Ru(2)–Ru(6)	87.2(1)	Ru(2)–Ru(6)–Ru(4)	91.6(1)	Ru(3)–B–Ru(6)	91.4(12)

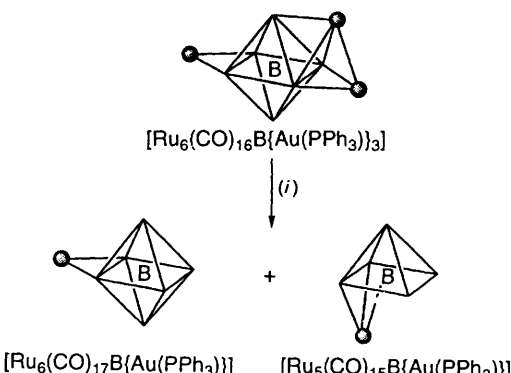
**Fig. 6** The 162 MHz  $^{31}\text{P}$  NMR spectrum of compound **6** at 180 K in  $\text{CD}_2\text{Cl}_2$  and the proposed fluxional process in solution

the  $\text{Ru}_6$  core with externally bound gold(I) phosphine groups leads to a significant lengthening of the bridged Ru–Ru edges; in **6**,  $\text{Ru}(1)\text{–Ru}(2)$  3.276(1) and  $\text{Ru}(3)\text{–Ru}(4)$  3.130(3)  $\text{\AA}$ . The boron atom in **6** is interstitially sited with Ru–B distances in the range 2.01–2.20  $\text{\AA}$ .

The  $\text{Ru}_6\text{BAu}_3\text{P}_3$  core of **6** is illustrated in Fig. 4(d). The positions of two of the three  $\text{Au}(\text{PPh}_3)$  units mimic those of the Group 11 metal units in  $[\text{Ru}_6(\text{CO})_{16}\text{C}(\text{Cu}(\text{NCMe}))_2]$ <sup>36</sup> and  $[\text{Ru}_5\text{W}(\text{CO})_{17}\text{C}(\text{Au}(\text{PEt}_3))_2]$ <sup>35</sup> [Fig. 4(c)] and are similar to the positions of those in the digold derivative **5**. The  $\text{Au}(1)\text{–Au}(2)$  distance is 2.899(2)  $\text{\AA}$ . Whereas in **5** the digold

unit lies symmetrically with respect to the  $\text{Ru}_6\text{B}$  core, in **6** the  $[\text{Au}(\text{PPh}_3)]_2$  unit is tilted so as to favour the  $\text{Ru}(6)\text{Ru}(1)\text{Ru}(2)$  face at the expense of the  $\text{Ru}(5)\text{Ru}(1)\text{Ru}(2)$  face as is seen in Fig. 5 [ $\text{Ru}(6)\text{–Au}(1)$  3.201(3) vs.  $\text{Ru}(5)\text{–Au}(2)$  3.328(1)  $\text{\AA}$ ]. The third  $\text{Au}(\text{PPh}_3)$  fragment bridges edge  $\text{Ru}(4)\text{–Ru}(5)$ , the corresponding edge to that occupied by the hydride ligand in **5**.

**Solution Properties of  $[\text{Ru}_6\text{H}(\text{CO})_{16}\text{B}\{\text{Au}(\text{PPh}_3)\}_2]$  and  $[\text{Ru}_6(\text{CO})_{16}\text{B}\{\text{Au}(\text{PPh}_3)\}_3]$ .**—Dynamic processes involving  $\text{M}(\text{PR}_3)$  units ( $\text{M}$  = Group 11 metal) in cluster molecules are well documented and it is generally considered that the  $\text{Au}(\text{PR}_3)$  unit remains intact during fluxionality.<sup>34,39,40</sup> Processes involving a ‘rocking’ motion of a digold unit with respect to a transition-metal core have been proposed in several instances, for example in the interconversion of isomers of clusters with  $\text{Ru}_4\text{Au}_2$  cores<sup>40</sup> and, in our own work, in  $[\text{Fe}_4(\text{CO})_{12}\text{BH}\{\text{Au}(\text{PR}_3)\}_2]$  ( $\text{R}$  = Ph or Et).<sup>41</sup> In the solid state the two  $\text{Au}(\text{PPh}_3)$  units in compound **5** are equivalent and in solution this equivalence is maintained as evidenced by the  $^{31}\text{P}$  NMR spectrum ( $\text{CDCl}_3$ , 298 K) which exhibits one sharp resonance. The  $^{31}\text{P}$  NMR spectrum of the trigold derivative **6** dissolved in  $\text{CD}_2\text{Cl}_2$  exhibits two sharp resonances at 298 K with integrals in a ratio 2:1. No changes are observed in the spectrum as the temperature is lowered to 180 K (Fig. 6). The solid-state structure of **6** [Figs. 4(d) and 5] possesses three inequivalent phosphorus environments. The observed variable-temperature  $^{31}\text{P}$  NMR spectra can be rationalised if the atoms  $\text{Au}(1)$  and  $\text{Au}(2)$  (with their associated phosphine ligands) participate in a fluxional process as illustrated in Fig. 6. This process would make atoms P(1) and P(2) equivalent while P(3) remains unaffected. The presence of a mirror plane in the solution structure of **6** is supported by  $^{13}\text{C}$  NMR spectroscopic data. At 298 K four  $^{13}\text{C}$  NMR spectral resonances are observed in the



Scheme 1 (i) 70 atm CO, 50 °C, CH<sub>2</sub>Cl<sub>2</sub>

carbonyl region of the spectrum at δ + 253.3, + 204.2, + 201.3 and + 197.9 with integrals 2:6:4:4 respectively. The signal at δ + 253.3 is assigned to two bridging carbonyl ligands, that at δ + 204.2 to the carbonyl ligands attached to atoms Ru(5) and Ru(6) (Fig. 5), and the two remaining signals to the eight CO ligands bonded to atoms Ru(1), Ru(2), Ru(3) and Ru(4). The solution data support the premise that, in addition to the fluxional process shown in Fig. 6, the carbonyl ligands centred on atoms Ru(5) and Ru(6) undergo localised site exchange while all other carbonyl ligands are static at 298 K.

**Reaction of [Ru<sub>6</sub>(CO)<sub>16</sub>B{Au(PPh<sub>3</sub>)<sub>3</sub>} with CO.**—The reaction of compound **6** with CO showed that two competitive pathways are operative. In the first, two gold(i) phosphine ligands in **6** are replaced by one carbonyl ligand to give **4**. The second route, which occurs preferentially, is the cleavage of one ruthenium vertex in addition to the loss of two gold(i) triphenylphosphine fragments to yield [Ru<sub>5</sub>(CO)<sub>15</sub>B{Au(PPh<sub>3</sub>)}] (Scheme 1). We have previously shown that the reaction of **4** with CO under similar conditions leads to this pentaruthenium boride cluster.<sup>29</sup>

## Conclusion

The reaction of [Ru<sub>3</sub>(CO)<sub>9</sub>(B<sub>2</sub>H<sub>5</sub>)]<sup>-</sup> with [Ru<sub>3</sub>(CO)<sub>10</sub>-(NCMe)<sub>2</sub>] leads, significantly, to both the octahedral and trigonal-prismatic boride cluster anions [Ru<sub>6</sub>(CO)<sub>17</sub>B]<sup>-</sup> and [Ru<sub>6</sub>H<sub>2</sub>(CO)<sub>18</sub>B]<sup>-</sup>, respectively, illustrating that the assembly of particular hexametal cages is not wholly controlled by the size of the interstitial atom. However, the products of reactions of [Ru<sub>6</sub>(CO)<sub>17</sub>B]<sup>-</sup> and [Ru<sub>6</sub>H<sub>2</sub>(CO)<sub>18</sub>B]<sup>-</sup> with the gold(i) phosphines [AuCl(PPh<sub>3</sub>)<sub>2</sub>] and [AuCl{P(C<sub>6</sub>H<sub>4</sub>Me-2)<sub>3</sub>}<sub>2</sub>] show a preference for an octahedral Ru<sub>6</sub>B cluster core. Mono-, di- and tri-gold derivatives are isolated but the best route to [Ru<sub>6</sub>(CO)<sub>16</sub>B{Au(PR<sub>3</sub>)<sub>3</sub>}] involves the reaction of [Ru<sub>6</sub>(CO)<sub>17</sub>B]<sup>-</sup> with [{(R<sub>3</sub>P)Au}<sub>3</sub>O]<sup>+</sup> (R = Ph or 2-MeC<sub>6</sub>H<sub>4</sub>).

## Acknowledgements

We thank the donors of the Petroleum Research Fund, administered by the American Chemical Society, for support of this work (grants Nos. 19155-AC3 and 22771-AC3), the SERC for studentships (to D. M. M. and A. W.) and the National Science Foundation for a grant (CHE 9007852) towards the purchase of a diffractometer at the University of Delaware. We acknowledge the help of Dr. Xuejing Song in preliminary work.<sup>18</sup>

## References

- J. S. Bradley, *Adv. Organomet. Chem.*, 1983, **22**, 1.
- E. L. Muettterties, *Prog. Inorg. Chem.*, 1981, **28**, 203.
- M. D. Vargas and J. N. Nicholls, *Adv. Inorg. Chem. Radiochem.*, 1986, **30**, 123.
- C. E. Housecroft, in *Modern Inorganic Chemistry*, ed. T. P. Fehlner, Plenum, New York, 1992, ch. 3, p. 73.
- W. L. Gladfelter, *Adv. Organomet. Chem.*, 1985, **24**, 41.
- V. G. Albano, M. Sansoni, P. Chini and S. Martinengo, *J. Chem. Soc., Dalton Trans.*, 1973, 651.
- S. Martinengo, G. Ciani, A. Sironi, B. T. Heaton and J. Mason, *J. Am. Chem. Soc.*, 1979, **101**, 7095.
- V. G. Albano, D. Braga and S. Martinengo, *J. Chem. Soc., Dalton Trans.*, 1986, 981.
- G. Ciani and S. Martinengo, *J. Organomet. Chem.*, 1986, **306**, C49.
- S. Martinengo, D. Strumolo, P. Chini, V. G. Albano and D. Braga, *J. Chem. Soc., Dalton Trans.*, 1985, 35.
- R. Bonfichi, G. Ciani, A. Sironi and S. Martinengo, *J. Chem. Soc., Dalton Trans.*, 1983, 253.
- R. Khattar, J. Puga, T. P. Fehlner and A. L. Rheingold, *J. Am. Chem. Soc.*, 1989, **111**, 1877.
- F.-E. Hong, T. J. Coffy, D. A. McCarthy and S. G. Shore, *Inorg. Chem.*, 1989, **28**, 3284.
- S. M. Draper, C. E. Housecroft, A. K. Keep, D. M. Matthews, X. Song and A. L. Rheingold, *J. Organomet. Chem.*, 1992, **423**, 241.
- A. K. Bandyopadhyay, R. Khattar, J. Puga, T. P. Fehlner and A. L. Rheingold, *Inorg. Chem.*, 1992, **31**, 465.
- S. B. Colbran, C. M. Hay, B. F. G. Johnson, F. J. Lahoz, J. Lewis and P. R. Raithby, *J. Chem. Soc., Chem. Commun.*, 1986, 1766.
- S. B. Colbran, F. J. Lahoz, P. R. Raithby, J. Lewis, B. F. G. Johnson and C. J. Cardin, *J. Chem. Soc., Dalton Trans.*, 1988, 173.
- C. E. Housecroft, D. M. Matthews, A. L. Rheingold and X. Song, *J. Chem. Soc., Chem. Commun.*, 1992, 842.
- A. K. Chipperfield, C. E. Housecroft and P. R. Raithby, *Organometallics*, 1990, **9**, 479.
- F. G. Mann, A. F. Wells and D. Purdie, *J. Chem. Soc.*, 1937, 1828; D. R. Williamson, *J. Inorg. Nucl. Chem.*, 1972, **34**, 3393.
- A. N. Nesmeyanov, E. G. Perevalova, Yu. T. Strukhov, M. Yu. Antipin, K. I. Grandberg and V. P. Dyadchenko, *J. Organomet. Chem.*, 1980, **201**, 343.
- S. R. Drake and R. Khattar, *Organomet. Synth.*, 1988, **4**, 234.
- C. E. Housecroft, D. M. Matthews, A. L. Rheingold and X. Song, *J. Chem. Soc., Dalton Trans.*, 1992, 2855.
- A. K. Chipperfield, C. E. Housecroft and D. M. Matthews, *J. Organomet. Chem.*, 1990, **384**, C38.
- F.-E. Hong, D. A. McCarthy, J. P. White, C. E. Cottrell and S. G. Shore, *Inorg. Chem.*, 1990, **29**, 2874.
- A. K. Chipperfield, C. E. Housecroft and A. L. Rheingold, *Organometallics*, 1990, **9**, 681.
- C. R. Eady, B. F. G. Johnson and J. Lewis, *J. Chem. Soc., Dalton Trans.*, 1977, 477.
- M. I. Bruce and B. K. Nicholson, *J. Organomet. Chem.*, 1983, **252**, 243.
- C. E. Housecroft, D. M. Matthews and A. L. Rheingold, *Organometallics*, 1992, **11**, 2959.
- (a) H. Hope and B. Moezzi, XABS, Department of Chemistry, University of California at Davis, CA; (b) G. Sheldrick, Siemens XRD, Madison, WI.
- T. P. Fehlner, *Adv. Organomet. Chem.*, 1990, **35**, 199 and refs. therein.
- N. Greenwood, R. V. Parish and P. Thornton, *Q. Rev. Chem. Soc.*, 1966, **20**, 441.
- See, for example, R. Khattar, T. P. Fehlner and P. T. Czech, *New J. Chem.*, 1991, **15**, 705.
- I. D. Salter, *Adv. Organomet. Chem.*, 1989, **29**, 249.
- S. R. Bunkhall, H. D. Holden, B. F. G. Johnson, J. Lewis, G. N. Pain, P. R. Raithby and M. J. Taylor, *J. Chem. Soc., Chem. Commun.*, 1984, 25.
- J. S. Bradley, R. L. Pruet, E. Hill, G. B. Ansell, M. E. Leonowicz and M. A. Modrick, *Organometallics*, 1982, **1**, 748.
- C. E. Housecroft and A. L. Rheingold, *J. Am. Chem. Soc.*, 1987, **6**, 1332.
- C. E. Housecroft, M. S. Shongwe and A. L. Rheingold, *Organometallics*, 1989, **8**, 2651.
- See, for example, J. A. K. Howard, I. D. Salter and F. G. A. Stone, *Polyhedron*, 1984, **3**, 567.
- A. G. Orpen and I. D. Salter, *Organometallics*, 1991, **10**, 111.
- K. S. Harpp and C. E. Housecroft, *J. Organomet. Chem.*, 1988, **340**, 389.

Received 28th May 1993; Paper 3/03056C